HHS Public Access

Author manuscript

Exp Neurol. Author manuscript; available in PMC 2019 November 01.

Published in final edited form as:

Exp Neurol. 2018 November ; 309: 91–106. doi:10.1016/j.expneurol.2018.07.016.

Increased expression of Toll-like Receptor 3, an Anti-Viral Signaling Molecule, and Related Genes in Alzheimer's Disease Brains

Douglas G. Walker[a,b,c,*], **Tiffany M. Tang**[b,**], and **Lih-Fen Lue**[b,c]

[a]Molecular Neuroscience Research Center, Shiga University of Medical Science, Otsu, Japan

[b]Neurodegenerative Disease Research Center, Biodesign Institute, Arizona State University, Tempe, Arizona, U.S.A

[C]Banner Sun Health Research Institute, Sun City, Arizona, U.S.A

Abstract

The focus of this study is the expression of Toll-like receptor-3 (TLR-3), a receptor for double-stranded RNA, in human brains affected by Alzheimer's disease (AD) pathology. Toll-like receptors are a family of pattern recognition molecules primarily involved in host defenses to microbial pathogens, but roles in neurodegenerative disease have also been shown, as amyloid beta (Aβ) can be a ligand for TLR-2 and −4 and α-synuclein for TLR-1 and TLR-2, while TLR-9 activation promotes Aβ removal. However, involvement of TLR-3 in AD has not been rigorously studied. Immunohistochemical analyses in human temporal cortical sections with a validated antibody for TLR-3 predominantly identified microglia, particularly strongly in cells associated with amyloid plaques, also brain vascular endothelial cells and subsets of astrocytes, but not neurons or p62-immunoreactive structures. Microglial TLR-3 colocalized with the endosomal/lysosomal marker CD68, which identifies phagocytic cells. Quantitative analyses of neuropathologically-staged human brain middle temporal gyrus samples using immunohistochemistry and mRNA expression methods demonstrated increased TLR-3 immunoreactivity and increased TLR-3 mRNA in AD compared to non-demented cases. There were significant positive correlations between TLR-3 mRNA levels and plaque or tangle loads in both series of samples. Increased expression of interferon beta (IFN-β) and interferon regulatory factor (IRF)-3 mRNA, two factors induced by TLR-3 signaling, were detected in the AD cases. Increased expression of TLR-4 and TLR-9 mRNA was also observed in these same samples, but not TLR-2. *In vitro* cultured human brain microglia responses to Aβ inflammatory activation were not altered by TLR-3 activation with activator polyinosinic;polycytidylic acid (poly I:C), while

*Corresponding Author: Dr. Douglas G. Walker, Molecular Neuroscience Research Center, Shiga University of Medical Science, Seta Tsukinowa-cho, Otsu, Shiga 520-2192, JAPAN, walker@belle.shiga-med.ac.jp.

**Current Address Biomedical Sciences Graduate Program, College of Medicine, Pennsylvania State University, Hershey, PA, U.S.A

human brain endothelial cells showed reduction in responses when stimulated with both agents. Treatment of microglia with poly I:C did not increase their uptake and breakdown of Aβ.

Keywords

Inflammation; neuropathology; phagocytosis; plaques; tangles; microglia; interferon responses; Immunohistochemistry

1. Introduction

Toll-like receptors (TLRs) in humans are a family of 10 pathogen-associated pattern recognition receptors mainly involved in host immunity to microbial pathogens and recognize different viral, bacterial and fungal nucleic acids, lipids or lipoproteins (O'Neill et al., 2013). Additional TLR ligands associated with cellular damage/death in the absence of infection have been identified (Vidya et al., 2017). TLRs are type I transmembrane receptors localized to plasma membranes or endolysosomal membranes with conserved molecular structures of ectodomains containing leucine-rich repeats. TLR-1, TLR-2, TLR-4, TLR-5, TLR-6 and TLR-10 are primarily localized to the plasma membrane, while TLR-3, TLR-7, TLR-8 and TLR-9 are mainly on intracellular endolysosomal vesicles. In addition to responding to microbial components, TLR responses to molecules associated with dying cells, such as oxidized low-density lipoprotein, oxidized phospholipids, β-defensin-2, highmobility group box 1, degradation products of extracellular matrix and heat shock proteins, and cellular RNA and DNA amongst others, have been shown (Leifer and Medvedev, 2016). Several TLRs can be activated by abnormal molecules associated with neurodegeneration, including TLR-2 and TLR-4 by amyloid beta (Aβ) (Balducci et al., 2017; Reed-Geaghan et al., 2009) and TLR-1 and TLR-2 by α-synuclein (Daniele et al., 2015; Kim et al., 2016). Activation of TLR-9, an endosome localized TLR, by its ligand unmethylated DNA has been shown to stimulate Aβ removal in different Alzheimer's disease (AD) animal models (Scholtzova et al., 2009, 2014, 2017). It has been hypothesized that TLR activation might enhance activity of phagocytic cells through stimulation of autophagy processes (Xu et al., 2008; Zhan et al., 2014). Colocalization of TLR-3 and autophagy markers was identified in thalamus neurons of preterm infants with white matter injury (Vontell et al., 2015).

Complex signaling pathways activated by TLRs have been defined, which result in inflammatory activation through the transcription factor NFκB or through activation of type 1 interferon (IFN) responses (Kawai and Akira, 2007a, 2007b; Takeuchi et al., 2004). All TLRs except TLR-3 use the adaptor protein myeloid differentiation response protein 88 (MyD88) as a signaling intermediate. By contrast, TLR-3, an endosomal-located receptor, whose native ligand is double-stranded RNA (dsRNA) primarily utilizes Toll-IL-1 receptor domaincontaining adaptor inducing IFN-β (TRIF) as an adaptor protein to activate signaling. TLR-3 activation is involved in cellular responses to a number of different viruses, including infection by the DNA herpes simplex virus, which results in a strong type 1 interferon antiviral response (Boivin et al., 2008; Majde et al., 2010; Nazmi et al., 2014; Wang et al., 2004). Although discounted for many years, recent studies have provided new

evidence of association of viruses, including human herpesvirus (HHV)-6A and −7 and hepatitis B virus, with AD pathology (Mastroeni et al., 2018; Readhead et al., 2018). Recent results showed that TLR-3 can be activated by different mRNA species (Kariko et al., 2004b), and even double stranded siRNA complexes (Kariko et al., 2004a). A unique non-nucleic acid ligand for TLR-3 was identified as stathmin, a microtubule-associated regulator cytoskeleton protein (Bsibsi et al., 2010). Stathmin is abundant in brain and was shown to activate TLR-3 signaling in human astrocytes and microglia in a similar manner to the artificial dsRNA ligand polyinosinic;polycytidylic acid (poly I:C).

Controlling innate inflammation due to enhanced TLR activation has been a therapeutic target for a number of diseases; however, with regards to TLR-3, there have been studies showing that enhanced TLR-3 signaling can have protective effects (Li et al., 2015; Zhou et al., 2015). The possible involvement of TLR-3 and type 1 beta interferon (IFN-β) responses in neuronal autophagy was demonstrated in PD animal models. Lack of IFN-β directly resulted in neurodegeneration and accumulation of α-synuclein in Lewy body like structures due to defects in autophagy (Ejlerskov et al., 2015).

TLR-3 expression has been demonstrated in many different cell types, but particularly in inflammatory cells with significantly increased expression in mature dendritic myeloid cells (Muzio et al., 2000). The increased expression of TLR-3 in monocyte-derived dendritic cells (DC) defined it as a marker for this cell type (Muzio et al., 2000). In brain, expression has been observed in microglia, astrocytes, endothelial cells and neurons (Bsibsi et al., 2006, 2002; Facci et al., 2014; Jack et al., 2007; Jeong et al., 2015; Li et al., 2013; Nagyoszi et al., 2010). A recent study showed that TLR-3 activation in neurons affected neuronal morphology and expression of genes involved in schizophrenia (Chen et al., 2017). Other studies have shown TLR-3 activation was involved in neurogenesis (Lathia et al., 2008; Okun et al., 2010). A recent review of TLRs in AD succinctly summarized roles for TLR-2, TLR-4 and TLR-9, but there have been no human brain tissue studies of TLR-3 involvement in AD neurodegeneration (Su et al., 2016)

Studies involving TLR-3 activation, primarily using poly I:C as ligand, have shown both damaging and protective effects. Direct injection of poly I:C into brain resulted in significant neurotoxicity in the substantia nigra through inflammatory activation (Deleidi et al., 2010). Similarly, intravenous administration of poly I:C to AD model mice increased Aβ deposition and phosphorylated tau pathology (Krstic et al., 2012). Treatment of astrocytes and microglia with poly I:C resulted in increased expression of pro-inflammatory and antiinflammatory cytokines depending on dose (Bsibsi et al., 2010, 2006), including a number of neuroprotective cytokines and growth factors. Involvement of TLR-3 signaling in the absence of virus infection has been established, and protective effects of enhanced TLR-3 signaling in cerebral ischemia and possibly multiple sclerosis have been identified (Pan et al., 2012; Shi et al., 2013; Wang et al., 2014).

The purpose of the studies in this report was to assess whether there might be involvement of TLR-3 in AD-related inflammatory pathology. The first stage was to identify cellular localization and gene expression in AD brains, and then to model findings using unique *in vitro* cellular models of microglia and brain endothelial cells derived from human aged

brains. We identified increased expression of TLR-3 associated with increasing amounts of AD pathology, but the changes in expression appeared to be late in the disease process. *In vitro* experiments showed that Aβ treatment did not induce TLR-3 expression by microglia.

2. Materials and Methods

2.1 Human brain tissue samples and diagnoses criteria

Human brain tissue samples used in this study were obtained from the Banner Sun Health Research Institute Brain and Body Donation Program (Beach et al., 2008, 2015). The operations of the Brain and Body Donation Program have been reviewed by an Institutional Review Board (Western IRB, Puyallup, WA). Summary of details of all cases used in this study are summarized in Table 1. The use of human tissues for experimentation had the approval of all institutions involved.

To assess severity of AD pathology in each case, tissue sections from 5 brain regions (entorhinal cortex, hippocampus, frontal cortex, temporal cortex and parietal cortex) were stained with Thioflavin S, Gallyas or Campbell-Switzer histological stains and assessed semi-quantitatively for the density of neurofibrillary tangles and amyloid plaques. Each brain region was ranked on a scale of 0–3. By combining the measures across these 5 brain regions, assessment of AD pathology was ranked on a non-parametric scale of 0–15 for plaques and tangles (Dugger et al., 2012). Two sets of cases were subdivided into nondemented low plaque (ND-LP)(plaque score < 6), non-demented high plaque (NDHP) (plaque score 6–12) and AD (plaque score > 12), while the third set was considered as ND (plaque scores < 5) and AD (plaque score > 12). Conventional consensus clinical and neuropathological criteria (e.g. Braak staging) were also used to diagnose AD, dementia with Lewy bodies (DLB) and Parkinson's disease (PD) in these cases (McKeith et al., 2005; Newell et al., 1999).

Tissue taken from the right hemisphere of each brain donor at autopsy was frozen on dry ice in 1 cm thick coronal slices, while 1 cm thick coronal slices from the left hemisphere were fixed for 2 days in formaldehyde followed by cryoprotection in phosphate buffered glycol/glycerol. Frozen brain slices were stored at −70 to −80oC, and retrieved for dissection when samples were required for biochemical studies.

Apolipoprotein E (apoE) genotypes were determined for all cases using a PCR restriction fragment polymorphism technique employing DNA extracted from cerebellum (Hixson and Vernier, 1990).

2.2 Immunohistochemistry

Formaldehyde-fixed tissue sections from middle temporal gyrus were used for cellular localization of TLR-3 alone, or with Aβ; microglia markers HLA-DR, Ionized calcium binding adaptor molecule (IBA-1) and CD68; astrocyte marker glial fibrillary acidic protein (GFAP); vascular endothelial marker CD31, neuronal marker NeuN and the autophagy associated receptor p62 according to our previously published procedures (Walker et al, 2009; 2015). Antibodies used in this study for immunohistochemistry and western blots are listed in Table 2. To detect TLR-3 immunoreactivity in fixed tissue sections, antigen retrieval

pretreatment was necessary. Each section was heated at 80oC for 30 minutes in 1 mM EDTA (pH 8.0) followed by cooling to room temperature. This antigen retrieval method did not affect the performance of the other antibodies used for double immunohistochemistry. Localization of bound antibody was visualized using avidin-biotinhorseradish peroxidase enzyme complex (ABC-Vector Laboratories, Burlingame, CA) histochemistry and nickel ammonium sulfate-enhanced diaminobenzidine (DAB) as substrate to produce a purple reaction product. The second round of histochemistry was carried out using various antibodies. For dual-color immunohistochemistry, binding of the second antibody was detected using the same procedure, but with DAB without nickel ammonium sulfate for substrate to produce a brown reaction product (Walker et al., 2009; Walker et al., 2015). Multi-color laser confocal microscopy was used in a limited number of cases to validate antigen localization. Sections were incubated overnight in antibodies, washed 3 times and incubated with mixtures of fluorescent-labelled secondary antibodies at 1:500 dilution. Antibodies were labeled with Alexa 488 (donkey anti goat IgG), Alexa 568 (donkey anti-rabbit or anti-mouse IgG) and Alexa 647 (donkey anti mouse IgG). After washing, sections were mounted and counterstained with 1% Sudan black (in 70% ethanol) to block autofluorescence. Sections were examined using Olympus FV1000 confocal microscope and images output using system software.

To confirm specificity of immunostaining, protein absorption of the goat polyclonal TLR-3 antibody was carried by mixing pre-diluted antibody with excess of recombinant TLR3 protein (Peprotech, Rocky Hill, NJ) for 18 hours prior to incubation of antibody/protein mixture on tissue sections. As a control, aliquots of diluted antibody without added TLR-3 protein were processed in parallel prior to use in immunohistochemistry.

2.3 Measurement of area occupied of TLR-3 immunoreactivity

Matched sections from each case from series A (ND-LP, ND-HP, and AD) were subjected to single color immunohistochemistry for TLR-3. For each stained section, 4 nonoverlapping fields were imaged at 4-times magnification to incorporate all cortical layers within a single field for each section. These images were quantified for area of immunoreactivity of TLR-3 using Image J analysis program (https://imagej.net/ImageJ). The mean area value for immunoreactivity in each section was calculated, and then these values were combined into the respective disease groups for statistical analysis.

2.4 Western Immunoblot and Immunoprecipitation Analyses

Detergent soluble extracts were prepared from brain tissues or cells by sonication in 5 volumes (weight to volume) of RIPA buffer (20 mM Tris-HCl, pH 7.5. 150 mM NaCl, 1% Triton X100, 1% sodium deoxycholate, 0.1 % sodium dodecyl sulfate) supplemented with protease and phosphatase inhibitors (Thermo Fisher Scientific). Total protein concentration of each sample was determined using a Micro BCA assay kit with bovine serum albumin as standard.

To assess the specificity of the TLR-3 antibodies (Table 2), protein extracts of human brain samples or transfected HEK cells were analyzed by standard western blot methodology with chemiluminescence detection (Walker et al., 2015). Immunoprecipitation was carried out

using protein G-conjugated magnetic beads (G-Biosciences, St. Louis, MO) conjugated with goat polyclonal antibody to TLR-3 (2 μg antibody/5 μl of beads). RIPAextracted brain or transfected cell extracts were reacted with TLR-3 antibody-conjugated beads for 2 hours, washed according the manufacturer's instructions, and eluted into gel sample buffer. Samples were separated by western blot procedures and probed with alternate TLR-3 antibodies.

2.5 Cell Culture Methods

Human autopsy brain microglia were isolated from frontal cortex according to our standard protocols (Walker et al., 2009; 2015a; 2015b). After isolation, microglia were cultured for 10–14 days prior to use in experiments. Microglia isolated from 8 separate cases were used in this study. We also isolated human brain endothelial cells (HBEC) from digested brain material by selection with *Ulex Europaeus* (UEA)-conjugated magnetic Dynabeads (Life Technologies). HBEC were cultured for 14–21 days using EGM-2 Endothelial Cell media (Lonza, Gaithersburg, MD) with the inclusion of puromycin (5 μg/ml) in the media for the first 2 days of culture to inhibit other cell types (Calabria et al., 2006). Microglia or HBEC were treated with preformed fibrils/oligomers of Aβ(1– 42) (California Peptide Company, Napa, CA) that had been aggregated according to our published procedure (Walker et al., 2006), or with different concentrations of poly I:C (Sigma Aldrich, St. Louis, MO).

A modification to the above procedure was carried out when the aim of the experiment was to determine if poly I:C treatment modulated the stimulating effects of Aβ treatment or modulated the phagocytosis and breakdown of Aβ. For these experiments, microglia or HBEC cells were treated with poly I:C (2 μg/ml) for 1 hr before addition of indicated doses of Aβ. For experiments whose aims were to measure intracellular levels of Aβ, at the end of the treatment period, microglia were rinsed with PBS and then treated for 5 min with 0.01% trypsin solution to remove surface bound Aβ. Cultures were then rinsed twice with PBS prior to lysis in RIPA buffer. These materials were used for western blot analyses. ELISA for CCL2/MCP-1 were carried out on microglial-conditioned media using reagent from R&D Systems (Minneapolis, MN) according to the manufacturer's instructions.

An *in vitro* blood brain barrier (BBB) cell model was employed using HBEC to test effects of poly I:C For this model, HBEC were plated at 50,000 cell/wells onto Cellagen collagen disc (MPBio, Santa Ana, CA) inserts using EGM2 endothelial cell media. Each insert was placed into a well of a 24-well plate containing 300 μl of media under the insert and 100 μl of media in the insert. The development of transendothelial electrical resistance (TEER) was measured using EndOhm chamber with EVOM resistance meter device (World Precision Instruments, Sarasota, FL). After 4–5 days, after high TEER had been obtained, treatments were added to media in the inserts. For all cell experiments, treatments were carried out for 24 hours.

Transient and stably-transfected HEK 293 cells were prepared using a TLR-3 expression or control plasmid (Genecopoeia, Gaithersburg, MD). The TLR-3 expression plasmid (Genecopoeia # EX-I3713-M02 in pReceiver-M02 vector), or control GFP plasmid were transfected into HEK cells for 48–72 hours with Lipofectamine 2000 according to the manufacturer's protocol, or stably transformed TLR-3 expressing colonies were selected

using G418. These materials were used in western blot and immunoprecipitation experiments to characterize the TLR-3 antibodies.

2.6 RNA isolation and Quantitative reverse transcription polymerase chain reaction (qPCR) analysis of mRNA expression.

RNA was prepared from human brain tissue samples and cultured cells (human microglia and brain endothelial cells) using RNAeasy Plus Mini kits (Qiagen, Valencia, CA) according to the manufacturer's protocol, with RNA integrity being measured with an Agilent Bioanalyzer and RNA 6000 Nano kits (Agilent, Santa Clara, CA). Samples used for qPCR had RIN values greater than 7.0. RNA from brain samples (0.5 μg) and cultured cell samples (0.2 μg) were reverse transcribed using the Quantitect reverse transcription kit (Qiagen). Appropriate numbers of no reverse transcriptase controls were prepared in parallel for each batch of samples. For qPCR, cDNA samples were amplified using Perfecta Fast Mix 2x reaction mixture (Quanta Biosciences, Gaithersburg, MD) supplemented with 1.25μM of Eva Green. The primers used for gene expression analyses in this project are listed in Table 3. QPCR was carried out using a Stratagene Mx3000p machine and abundance of gene expression quantified relative to a standard curve. All PCR values were normalized against values for β-actin mRNA expression (Walker et al., 2009; Walker et al., 2015). QPCR analyses followed most of the recommended criteria for Minimum Information for Publication of Quantitative Real-Time PCR Experiment (MIQE) (Bustin et al., 2009).

2.7 Data Analysis

Data for relative changes with disease classification were analyzed by one-way analysis of variance (ANOVA) with Newman-Keuls post-hoc test for significance between paired groups. Determinations of the relationship between levels of TLR-3 and other genes studied and plaque scores and tangle scores were performed using Spearman correlation analysis. Significant differences were assumed if p values of less than 0.05 were obtained. All statistical analyses were carried out using Graphpad Prism Version 7 software.

3. Results

3.1. Validation of antibodies to TLR-3

The initial basis of this study was the demonstration of cellular localization of immunoreactivity using a goat polyclonal antibody to TLR-3 (R&D Systems – AF1487) in formaldehyde-fixed brain sections. As listed in Table 2, different TLR-3 antibodies were tested or used in aspects of this study, but the goat polyclonal antibody was the only one giving positive results by immunohistochemistry on our brain tissue sections. The finding of predominant localization to microglia and lack of neuronal staining in tissue sections was different from other reports. Also, since this antibody produced a major band of 130 kDa by western blot with brain samples, a molecular weight greater than commonly reported for TLR-3 in other cell types, the specificity of this antibody was validated using different approaches.

Firstly, a comparison was made between a mouse monoclonal antibody to TLR-3 (R&D Systems – MAB1487) with the goat polyclonal as both antibodies were prepared using the

same eukaryotic cell-expressed proteins. Protein extracts of HEK cells transfected with a TLR-3 expressing or control plasmid were analyzed on western blots in comparison with human brain samples (supplemental Fig.1). Comparing the mouse monoclonal antibody (supplemental Fig. 1A) with the goat polyclonal (supplemental Fig. 1B) showed that the transfected cell expressed TLR-3 had higher molecular weight to human brain TLR-3, but the mouse monoclonal identified recombinant expressed TLR-3 at high affinity, but only weakly recognized brain TLR-3. The goat polyclonal antibody reacted with recombinant expressed TLR-3, but had stronger reactivity with brain TLR-3 (supplemental Fig. 1B). TLR-3 is extensively glycosylated, and this could be responsible for the different antibody properties and molecular weights between HEK-expressed TLR-3 and brain TLR-3. As follow-up, immunoprecipitation analyses were carried out with recombinant expressed TLR-3 and control materials (supplemental Fig. 1C), and human brain extracts (supplemental Fig. 1D) to confirm specificity. Both brain and recombinant expressed samples were immunoprecipitated with the goat polyclonal antibody to TLR-3, and detected by western blotting with alternate TLR-3 antibodies (supplemental Fig. 1C – mouse monoclonal; and supplemental Fig. 1D – rabbit polyclonal (ab62566)). These results showed that the goat polyclonal antibody precipitated proteins of approximately 130 kDa, which were recognized by these other antibodies. Finally, direct western blot comparison was carried out with brain samples from different brain regions. The blots were probed with the goat polyclonal (supplemental Fig. 1E), rabbit polyclonal (ab62566) (supplemental Fig. 1F) and rabbit polyclonal (Thermo-Fisher PA5–23510) (supplemental Fig. 1G). Although the latter two antibodies detected the same major protein bands as the goat polyclonal antibody, neither could produce specific immunoreactivity on fixed brain tissue sections (data not shown).

3.2. Distribution of TLR-3 immunoreactivity in human middle temporal gyrus

The initial observation for this project was the distinct TLR-3 immunoreactivity in cells associated with AD plaques. Immunoreactivity was noticeable in control aged (ND) brains with some plaque pathology, but there was distinct increase in the AD-affected brains. Immunoreactivity for TLR-3 was identified in microglia (Fig. 1) in ND low plaque (ND-LP) (Fig.-1A), ND high plaque (ND-HP) (Fig. 1B) and AD (Fig. 1C) tissue sections. These sections show double staining with TLR-3 (purple) and the microglial marker IBA-1 (brown). Most of the microglia in all of the examined sections showed some TLR-3 immunoreactivity, irrespective of their activation morphology, but there was distinct increase in intensity of immunoreactivity in microglia with activated morphology, particularly in the AD cases. Double staining for TLR-3 and the astrocyte marker GFAP showed some astrocytes were TLR-3 positive, but this was only observed in a small subset of these cells in both ND and AD cases (Fig. 1D-F). Many CD31-positive vascular endothelial cells also showed immunoreactivity for TLR-3 (Fig. 1G-I), but without noticeably increased immunoreactivity in vessels of AD cases (Fig. 1I). In all sections, strong TLR-3 immunoreactivity was observed in plaque-associated cells (Fig. 1 J-L). This TLR-3 plaque-associated immunoreactivity was an early event as it was observable even in the few plaques present in the ND-LP cases (Fig. 1J).

Colocalization of antigens was validated in some of the cases using multi-color confocal microscopy (Fig. 2). Examples shown in figure are for AD cases where TLR-3 immunoreactivity was strongest. To confirm microglial expression of TLR-3, sections were stained with TLR-3 and IBA-1. The individual and merged images show punctate immunoreactivity for TLR-3 (Fig. 2 A-C). The next series showed that TLR-3 immunoreactivity predominantly colocalized with the endosomal/lysosomal marker CD68, which is most highly expressed in phagocytic microglia (Fig. 2 D-F). Some separation of color can be seen in the merged image (Fig. 2F) to show that colocalization of these markers was not complete. The next series showed colocalization of TLR-3 and Aβ on a plaque (Fig. 2 G-I). The merged image shows almost no yellow color indicating that Aβ was not present in TLR-3 positive endosome/lysosome structures. Colocalization of TLR-3 (green), IBA-1 (red) and Aβ (blue) shows an example of strong TLR-3 immunoreactivity in microglialassociated with plaques (Fig. 2 J-L). These images also show prominent vascular expression of TLR-3. The final series (Fig. 2 M, N, O) indicate limited TLR-3 colocalization with activated GFAP-positive astrocytes (Fig. 2M), and absence of TLR-3 with NeuN-positive neurons (Fig. 2N) or p62 positive structures (Fig. 2O).

3.3. Further Characterization of TLR-3 tissue immunoreactivity

The following control experiments were carried out to confirm observed TLR-3 immunoreactivity (supplemental Fig. 2). Pre-absorption of the goat polyclonal antibody with purified recombinant TLR-3 followed by immunohistochemistry with brain sections did not reveal the characteristic TLR-3 immunoreactivity (supplemental Fig. 2A and 2C). This was compared to sections treated with non-protein absorbed antibody, which showed the expected pattern of immunoreactivity (supplemental Fig 2. B and D). To confirm that double-stained sections with TLR-3 (purple) and the microglia marker HLA-DR were plaqueassociated, a selection of double-stained AD sections (supplemental Fig. 2E and 2F) were counterstained with Thioflavin S. The photomicrographs of Thioflavin S reactivity taken with fluorescent microscopy were recorded in the same position as for the light images. We also carried out TLR-3 immunoreactivity of a number of cerebellum sections as this brain region had been shown to have TLR-3 expression in neurons and Bergmann glia. This brain area does not tend to show AD pathology. A distinct pattern of immunoreactivity was observed in all sections with varying intensity (Fig 2G – ND; Fig. 2H – AD) in cells at the boundary of the molecular and granular cell layers. TLR-3 immunoreactive cells surrounded Purkinje neurons, but there was no evidence of positive staining of Purkinje neurons in any sections.

3.4. Quantitative analysis of TLR-3 immunoreactivity

To confirm increased TLR-3 immunoreactivity in AD brains, a series of sections from ND-LP, ND-HP and AD cases were immunostained, and the areas occupied by TLR-3 immunoreactivity measured using ImageJ analysis program. The results showed a significant increase in AD compared to ND-LP and ND-HP cases for area of TLR-3 immunoreactivity (Fig. 3A). Correlation analyses of these measures with the total brain plaque and tangle scores showed that TLR-3 area of immunoreactivity correlated positively with plaque scores (Spearman r=0.464, p=0.005) and tangle score (Spearman r=0.561, p=0.0005). The representative low magnification images of ND-LP (Fig. 3D), ND-HP (Fig. 3E) and AD

(Fig. 3F) show the change in distribution of TLR-3 immunoreactivity with increased pathology. There appeared to be increased expression in cortical layer V in AD cases compared to more restricted expression in layers I-III.

3.5. Expression of mRNA for TLR-3 and associated signaling molecules with increasing AD pathology

RNA and cDNA were prepared from two series of human brain MTG samples for gene expression analyses (Table 1). Samples in the first series were separated into ND and AD cases. The ND cases were selected for low plaque scores, and did not include ND-HP cases. A second series of MTG samples were analyzed for confirmation that included NDHP samples, with the goal of assessing TLR-3 expression changes with progression of pathology. In both series of RNA samples, we showed significantly increased expression of TLR-3 mRNA in AD cases (Fig. 4A and 4D). Correlation analyses between TLR-3 mRNA levels and total plaque or tangle scores showed significant positive correlation for both in the first series of samples (Fig. 4B and 4C), and with plaque scores, but not tangle scores, for the second series (Fig. 4E).

Expression of mRNA for interferon alpha (IFN-α), IFN-β, and interferon regulatory factor-3 (IRF-3), molecules associated with increased TLR-3 signaling, were also measured in the first series of samples (Fig. 5 A-C). Increased expression of IFN-β mRNA was detected in the AD series (Fig. 5B, $p<0.05$), but not for IFN-α (Fig. 5A). We also showed significantly increased expression of IRF-3 mRNA in the AD series (Fig. 5C), but not IRF-7 mRNA (data not shown). There were significant positive correlations between IRF-3 mRNA levels and plaque scores (Fig. 5D, Spearman $r=0.36$, $p=0.016$), and with tangle scores (Fig. 5E, Spearman $r=0.44$, $p=0.0034$). Correlation analyses were also carried out between TLR-3, IFN-β, and IRF-3 mRNA expression for these human brain samples. There were significant positive correlations between TLR-3 and IRF-3 mRNA levels (Pearson $r = 0.53$, $p=0.0005$), and between IFN-β and IRF-3 mRNA levels (Pearson $r = 0.48$, $p=0.0015$), but not between TLR-3 and IFN-β mRNA levels.

3.6. Expression of additional disease-associated TLR genes in AD

As involvement of other TLRs have been demonstrated in AD, in order to validate the samples being used, we determined whether disease-associated changes in mRNA expression could be detected for TLR-2, TLR-4, and TLR-9. Gene expression analysis showed significantly increased expression for TLR-4 and TLR-9 mRNA in AD cases (Fig. 6B and Fig. 6C), but not TLR-2 mRNA (Fig. 6A). There was strong positive correlation between TLR-9 mRNA expression and plaque (Spearman $r=0.5$, $p=0.0007$) and tangle scores ($r=0.53$, $p=0.0003$).

3.7. In vitro studies of TLR-3 activation in human microglia and human brain endothelial cells

Human postmortem brain-derived microglia, primarily from ND cases, were used to investigate features of TLR-3 activation. Treatment of microglia with increasing doses of aggregated Aβ (1–42) did not significantly increase expression of TLR-3 mRNA. By comparison, a biphasic response to poly I:C was observed in these cells. At the lowest dose,

TLR-3 mRNA expression was significantly inhibited, while at the highest dose TLR-3 mRNA expression was significantly increased by approximately 2-fold (Fig. 7A). Treatment of microglia with an intermediate dose of poly I:C (2.5 μg/ml) significantly increased expression of IFN-β, while co-treatment with Aβ (2 μM) produced no significant effect (Fig. 7B). Poly I:C treatment of microglia also significantly increased mRNA expression of the Aβ degrading enzyme neprilysin (MME), while co-treatment with Aβ did not alter this (Fig. 7C). Poly I:C or Aβ did not induce expression of insulin degrading enzyme (IDE) (Fig. 7D). To assess the effect of TLR-3 activation on microglia, secretion of the proinflammatory chemokine CCL2 (also known as monocyte chemoattractant protein-1 – MCP-1) was measured by ELISA in the media of treated cultures. Strong induction of CCL2 secretion was observed with the lowest dose (0.25 μg/ml) of poly I:C, but not at the higher doses (Fig. 7E). Treatment of microglia with aggregated Aβ (1–42) (2 μM) resulted in stronger induction of CCL2 than poly I:C (2.5 μg/ml). Co-treatment of cells with both agents did not significantly alter the secretion of CCL2 (Fig. 7F)

A different pattern of results was obtained following activation of brain endothelial cells with poly I:C. Poly I:C had a highly significant affect on properties of brain endothelial cells. For example, treatment of HBEC cultured on semi-permeable membranes in an *in vitro* blood brain barrier model with poly I:C resulted in significant reduction in transendothelial electrical resistance (TEER), a measure of the tightness of cellular interactions. Significant reduction in TEER occurred with treatment with the lowest dose (0.25 μg/ml), which was only further reduced marginally with higher doses (Fig. 8A). Treatment of HBEC with poly I:C (2.5 μg/ml) resulted in strong induction (11-fold) of TLR-3 mRNA expression, compared to the same dose for microglia (Fig. 8B) while co-treatment of cells with Aβ (2 μM) caused significant inhibition of this stimulation. A similar effect was observed for IFN-β mRNA expression (Fig. 8C), though similar to microglia, poly I:C and Aβ treatments did not affect expression of IDE mRNA (Fig. 8D).

We measured the levels of cell-associated Aβ present in microglia after 24 hours in the presence and absence of co-treatment with poly I:C. Poly I:C pretreatment did not affect the metabolism and breakdown of monomeric (Fig. 9A) or aggregated (Fig. 9B) Aβ. A representative western blot for these experiments are shown in Fig 9C.

4. Discussion

In this report, we present the first detailed investigation of TLR-3 expression in AD brains and show increased levels of TLR-3 mRNA and immunoreactivity, and increased IRF3 and IFN-β mRNA expression in AD. One previous study had identified TLR-3 expression in Bergmann glia in cerebellar cortex of AD cases, which was similar to our observations in this paper (supplemental Fig. 2 panels I and J) (Jackson et al., 2006). This previous publication identified TLR-3 immunoreactivity in Purkinje neurons only in cases with rabies and herpes virus encephalitis, but did not examine brain regions that are affected by AD pathology (Jackson et al., 2006). MTG was selected for our study as this brain region becomes significantly affected by AD pathology, while cerebellum does not, and matched series of frozen and fixed brain samples were available for most cases. Neuronal expression of TLR-3 has been reported in the periventricular white matter and ventral posterior

thalamus of samples of brains from pre-term infants (Vontell et al., 2013, 2015). TLR-3 staining in these studies was mainly in neurons and a subset of astrocytes, not microglia. Expression was significantly upregulated in cases with white matter injury. These studies utilized one of the TLR-3 antibodies (ab62566) that we had tested on our tissue. This antibody did not identify any structures in elderly brain tissues using our protocols. In the tissue samples examined in this study, we showed that TLR-3 immunoreactivity was primarily localized to microglia, but was also present in vascular endothelial cells and subsets of astrocytes We could not identify TLR-3 immunoreactivity in NeuN positive neurons in MTG. It is possible that the apparent cellular localization of TLR-3 does depend on the specificity of antibodies to antigenically distinct forms of TLR-3 due to differential glycosylation produced by different cell types.

Although we used a single antibody to TLR-3 to identify cellular localization of TLR-3, this antibody was the only one that showed this specific localization by immunohistochemistry in the fixed tissue samples available for this study. It does have unique features as the TLR-3 antibody (R&D Systems, AF1847) was the only one prepared using a eukaryotic cell-expressed protein covering the majority of the TLR-3 molecule, and thus should recognize multiple TLR-3 glycosylated epitopes. The other commercial TLR-3 polyclonal antibodies tested were raised against short synthetic (unglycosylated) peptide sequences. We showed that the R&D TLR-3 polyclonal antibody could recognize brainexpressed TLR-3 strongly, but was less effective at recognizing recombinant expressed TLR-3 compared to the R&D systems TLR-3 monoclonal antibody. By comparison, the monoclonal only weakly detected brain TLR-3. Further studies are required to characterize the differences between forms of TLR-3, but it is reasonable to hypothesize that this is due to differing degrees of glycosylation. Unlike other studies, this antibody only identified TLR-3 in cerebellum, not temporal cortex, neurons. Brain TLR-3 had a slightly smaller molecular weight than HEK cell-expressed recombinant TLR-3. Two other antibodies to TLR-3 recognized the full-length TLR-3 polypeptide as well as other bands by western blot. Three of the commercial antibodies could not recognize full-length TLR-3 in brain by western blot and were not further characterized. The validation of the goat polyclonal R&D antibody by detection of full-length brain and recombinant TLR-3 protein by western blot and immunoprecipitation, and by protein absorption of immunohistochemistry staining, established its specificity. One question has arisen about the discrepancy between our findings and reported molecular weight of TLR-3 as it has been widely reported that TLR-3 protein has a molecular weight of around 100 kDa. The detection of higher molecular weight full-length forms was unexpected, but we also noticed the presence of the 100 kDa form in brain and recombinant samples (supplemental Fig. 1). A recent study using airway epithelial cells report similar molecular weights for full length TLR3, and identified full-length TLR-3 polypeptides having molecular weights from 100–130 kDa (Duffney et al., 2017). Previous studies have shown that TLR-3 needs to be cleaved to form the active molecule (Garcia-Cattaneo et al., 2012; Toscano et al., 2013; Wang et al., 2014), suggesting that the presence of multiple TLR-3 immunoreactive peptide binds were consistent with its biological function.

4.1 Cellular localization and expression of TLR-3 in brain

The demonstration of TLR-3 expression by microglia and endothelial cells *in vivo* appears consistent with the well-established roles for TLRs in inflammatory responses. Expression of TLR-3 and functional responses by human microglia to TLR-3 ligand has previously been demonstrated (Bsibsi et al., 2002, 2010; Jack et al., 2007). Similarly, brain endothelial cells have been demonstrated to express TLR-3 mRNA (Li et al., 2013; Nagyoszi et al., 2010). Both cell types are involved in inflammatory responses in brain in many diseases. In blood-derived monocytic cells, expression of TLR-3 mRNA was restricted to monocyte-derived dendritic cells (Muzio et al., 2000). The lack of detection of neuronal staining in this study could be due to differences in specificity of antibodies, or the brain regions being studied. Most gray matter microglia throughout the MTG of ND-LP cases showed TLR-3 immunoreactivity, which became increased with increasing amounts of plaque pathology of ND-HP and AD cases. Plaque-associated microglia were strongly immunoreactive for TLR-3 in all disease groups. This was demonstrated quantitatively and using semi-quantitative immunohistochemistry analyses. Confocal fluorescent microscopy was carried out to confirm the findings by dual-color DAB immunohistochemistry. These findings confirmed the punctate pattern of TLR-3 in microglia, and strong staining in microglia associated with Aβ plaques. We further confirmed limited expression by activated microglia, and absence of expression by neurons. It was noticeable that only a subset of astrocytes were positive for TLR-3, while vessel endothelial staining was widespread feature in all cases. We also observed no colocalization of TLR-3 with the autophagy receptor p62, which strongly labeled tangles. If TLR-3 activation was stimulating or inhibiting autophagy and proteosomal degradation of peptide, colocalization of these proteins would be expected.

There were significantly increased expression of TLR-3 mRNA in AD in two separate series of cases. This increased expression significantly correlated positively with brain plaque and tangle loads. Evidence for increased TLR-3 signaling in AD was indirect, but we showed increased expression of IFN-β and IRF-3 mRNA in AD brains. TLR-3 mRNA levels correlated with levels of IRF-3, while IRF-3 and IFN-β mRNA levels showed significant correlation. Induction of IRF-3 has been shown to have an anti-inflammatory role in microglia *in vitro* by activating AKT/PI3 signaling pathway (Tarassishin et al., 2011). We also made some significant observations on TLR-3 localization and responses to poly I:C in brain endothelial cells. Brain endothelial expression of TLR 2, 3, 4, 6, and 9 has been identified, though not directly in human brains (Bhargavan and Kanmogne, 2018; Nagyoszi et al., 2010). The mRNA expression values for TLR-3, IRF-3 and IFN-β would be contributed by endothelial cells in tissue samples. TLR-3 expression by brain vascular endothelial cells *in vivo* provides a mechanism for the interaction of the brain vascular with the periphery, including viruses. Similar to our finding, it was observed that brain endothelial cells in culture react strongly to TLR-3 stimulation by upregulating its expression. (Bhargavan and Kanmogne, 2018). Based on qualitative observation, there was not a noticeable difference in expression of TLR-3 in vessels of AD cases compared to the ND cases. Further studies of tissue sections with appropriate methodology may be warranted to determine if TLR-3 expression by endothelial cells correspond with evidence of vascular dysfunction, a wellestablished feature of AD pathology.

4.2 TLR-3 expression and activation of brain-derived cells

In vitro experiments with human brain-derived microglia and endothelial cells demonstrated that aggregated Aβ(1–42) peptide alone did not significantly induce TLR-3 expression. The magnitude of responses of these cells to poly I:C for induction of TLR-3 was different. We noticed that there was a biphasic response of microglia to poly I:C depending on the dose used. At present, we do not know if TLR-3 has a physiological function in human brains, but induction of TLRs have generally only occurred in response to inflammatory stimuli. One study did show that TLR-3 activation of human astrocytes with a high dose poly I:C (50 μg/ml) induced both neuroprotective and pro-inflammatory cytokines (Bsibsi et al., 2006). The recent reappraisal of the role of viruses in AD pathology may be of direct relevance for TLR-3 activation in brain (Readhead et al., 2018).

A central feature of the *in vitro* experiments was to determine if stimulation of TLR-3 might affect cellular responses to Aβ. It was hypothesized that induction of a type I interferon response might modulate the responses by microglia to Aβ or similar stimuli. This could not be demonstrated for microglia, but was a feature for endothelial cell responses. TLR-3 stimulation did not directly affect microglia uptake or breakdown of Aβ, or affect expression of enzymes involved in Aβ degradation. The consequence of activation of TLR-3 in endothelial cells has been demonstrated in a transgenic AD mouse model study. Intravenous administration of poly I:C to 3xTgAD mice resulted in significantly enhanced plaque deposition and increased levels of phosphorylated tau. The mechanism for these findings is unclear but could be the consequence of weakening of the BBB by systemic poly I:C treatment combined with enhanced peripheral inflammation (Krstic et al., 2012). We did show significant reduction of BBB in vitro due to the actions of even a low dose of poly I:C. A similar enhancement in neurodegeneration was observed in prion-infected mice that were administered poly I:C. Increased neurodegeneration and microglial activation was observed in these mice even though there was increased expression of IFNα, IFNβ, IL-10, and TREM-2 (Field et al., 2010).

5. Conclusion

In summary, it was seen that TLR-3 is constitutively expressed by brain microglia and becomes upregulated with increasing amounts of AD pathology. The increased localization of TLR-3 expressing microglia associated with plaques would suggest a response to the plaque material, but we could not demonstrate upregulated expression of TLR-3 *in vitro* cultured microglia with Aβ treatment. With the recent evidence of viruses possibly being involved in AD (Readhead et al., 2018), it may be timely to consider TLR-3 and other related classes of anti-viral immune response proteins in AD inflammatory responses. Further studies will need to consider viruses and alternative ligands for inducing and activating TLR-3 in AD brains.

Supplementary Material

Refer to Web version on PubMed Central for supplementary material.

Acknowledgements

This work was supported by a grant National Institutes of Health, National Institutes on Aging (1R21AG044068) to DGW. DGW position at SUMS funded by institution. We thank the assistance of Dr. Thomas Beach, Dr. Geidy Serrano and Ms. Lucia Sue for providing the brain tissue samples for this study. The human brain samples were from the Banner Sun Health Research Institute Brain and Body Donation Program. The operation of the Banner Sun Health Research Institute Brain and Body Donation Program has been supported by the National Institute of Neurological Disorders and Stroke (U24 NS072026 National Brain and Tissue Resource for Parkinson's Disease and Related Disorders), the National Institute on Aging (P30 AG19610 Arizona Alzheimer's Disease Core Center), the Arizona Department of Health Services (contract 211002, Arizona Alzheimer's Research Center), the Arizona Biomedical Research Commission (contracts 4001, 0011, 05–901 and 1001 to the Arizona Parkinson's Disease Consortium) and the Michael J. Fox Foundation for Parkinson's Research (The Prescott Family Initiative).

References

Balducci C, Frasca A, Zotti M, La Vitola P, Mhillaj E, Grigoli E, Iacobellis M, Grandi F, Messa M, Colombo L, Molteni M, Trabace L, Rossetti C, Salmona M, Forloni G, 2017 Toll-like receptor 4-dependent glial cell activation mediates the impairment in memory establishment induced by beta-amyloid oligomers in an acute mouse model of Alzheimer's disease. Brain. Behav. Immun 60, 188–197. 10.1016/j.bbi.2016.10.012 [PubMed: 27751869]

Beach TG, Adler CH, Sue LI, Serrano G, Shill HA, Walker DG, Lue L, Roher AE, Dugger BN, Maarouf C, Birdsill AC, Intorcia A, Saxon-Labelle M, Pullen J, Scroggins A, Filon J, Scott S, Hoffman B, Garcia A, Caviness JN, Hentz JG, Driver-Dunckley E, Jacobson SA, Davis KJ, Belden CM, Long KE, Malek-Ahmadi M, Powell JJ, Gale LD, Nicholson LR, Caselli RJ, Woodruff BK, Rapscak SZ, Ahern GL, Shi J, Burke AD, Reiman EM, Sabbagh MN, 2015 Arizona Study of Aging and Neurodegenerative Disorders and Brain and Body Donation Program. Neuropathology 35, 354–89. 10.1111/neup.12189 [PubMed: 25619230]

Beach TG, Sue LI, Walker DG, Roher AE, Lue L, Vedders L, Connor DJ, Sabbagh MN, Rogers J, 2008 The Sun Health Research Institute Brain Donation Program: description and experience, 1987–2007. Cell Tissue Bank. 9, 229–45. 10.1007/s10561-008-9067-2 [PubMed: 18347928]

Bhargavan B, Kanmogne GD, 2018 Toll-Like Receptor-3 Mediates HIV-1-Induced Interleukin-6 Expression in the Human Brain Endothelium via TAK1 and JNK Pathways: Implications for Viral Neuropathogenesis. Mol. Neurobiol 55, 5976–5992. 10.1007/s12035-017-0816-8 [PubMed: 29128906]

Boivin N, Sergerie Y, Rivest S, Boivin G, 2008 Effect of pretreatment with toll-like receptor agonists in a mouse model of herpes simplex virus type 1 encephalitis. J. Infect. Dis 198, 664–672. 10.1086/590671 [PubMed: 18662130]

Bsibsi M, Bajramovic JJ, Vogt MHJ, van Duijvenvoorden E, Baghat A, Persoon-Deen C, Tielen F, Verbeek R, Huitinga I, Ryffel B, Kros A, Gerritsen WH, Amor S, van Noort JM, 2010 The microtubule regulator stathmin is an endogenous protein agonist for TLR3. J. Immunol 184, 6929–6937. 10.4049/jimmunol.0902419 [PubMed: 20483774]

Bsibsi M, Persoon-Deen C, Verwer RWH, Meeuwsen S, Ravid R, Van Noort JM, 2006 Toll-like receptor 3 on adult human astrocytes triggers production of neuroprotective mediators. Glia 53, 688–695. 10.1002/glia.20328 [PubMed: 16482523]

Bsibsi M, Ravid R, Gveric D, van Noort JM, 2002 Broad expression of Toll-like receptors in the human central nervous system. J. Neuropathol. Exp. Neurol 61, 1013–1021. [PubMed: 12430718]

Bustin SA, Benes V, Garson JA, Hellemans J, Huggett J, Kubista M, Mueller R, Nolan T, Pfaffl MW, Shipley GL, Vandesompele J, Wittwer CT, 2009. The MIQE guidelines: minimum information for publication of quantitative real-time PCR experiments. Clin. Chem 55, 611–622. 10.1373/clinchem.2008.112797 [PubMed: 19246619]

Calabria AR, Weidenfeller C, Jones AR, de Vries HE, Shusta EV, 2006 Puromycinpurified rat brain microvascular endothelial cell cultures exhibit improved barrier properties in response to glucocorticoid induction. J. Neurochem 97, 922–933. 10.1111/j.1471-4159.2006.03793.x [PubMed: 16573646]

Chen C-Y, Liu H-Y, Hsueh Y-P, 2017 TLR3 downregulates expression of schizophrenia gene Disc1 via MYD88 to control neuronal morphology. EMBO Rep. 18, 169–183. https://doi.org/10.15252/embr.201642586 [PubMed: 27979975]

Daniele SG, Beraud D, Davenport C, Cheng K, Yin H, Maguire-Zeiss KA, 2015 Activation of MyD88-dependent TLR1/2 signaling by misfolded alpha-synuclein, a protein linked to neurodegenerative disorders. Sci. Signal 8, ra45 10.1126/scisignal.2005965 [PubMed: 25969543]

Deleidi M, Hallett PJ, Koprich JB, Chung C-Y, Isacson O, 2010 The Toll-like receptor-3 agonist polyinosinic:polycytidylic acid triggers nigrostriatal dopaminergic degeneration. J. Neurosci 30, 16091–16101. 10.1523/JNEUROSCI.2400-10.2010 [PubMed: 21123556]

Duffney PF, McCarthy CE, Nogales A, Thatcher TH, Martinez-Sobrido L, Phipps RP, Sime PJ, 2017 Cigarette Smoke Dampens Anti-viral Signaling in Small Airway Epithelial Cells by Disrupting TLR3 Cleavage. Am. J. Physiol. Lung Cell. Mol. Physiol 10.1152/ajplung.00406.2017

Dugger BN, Serrano GE, Sue LI, Walker DG, Adler CH, Shill HA, Sabbagh MN, Caviness JN, Hidalgo J, Saxon-Labelle M, Chiarolanza G, Mariner M, HenryWatson J, Beach TG, 2012 Presence of Striatal Amyloid Plaques in Parkinson's Disease Dementia Predicts Concomitant Alzheimer's Disease: Usefulness for Amyloid Imaging. J. Parkinsons. Dis 2, 57–65. 10.3233/JPD-2012-11073 [PubMed: 22924088]

Ejlerskov P, Hultberg JG, Wang J, Carlsson R, Ambjorn M, Kuss M, Liu Y, Porcu G, Kolkova K, Friis Rundsten C, Ruscher K, Pakkenberg B, Goldmann T, Loreth D, Prinz M, Rubinsztein DC, Issazadeh-Navikas S, 2015 Lack of Neuronal IFN-beta-IFNAR Causes Lewy Body- and Parkinson's Disease-like Dementia. Cell 163, 324–339. 10.1016/j.cell.2015.08.069 [PubMed: 26451483]

Facci L, Barbierato M, Marinelli C, Argentini C, Skaper SD, Giusti P, 2014 Toll-like receptors 2, −3 and −4 prime microglia but not astrocytes across central nervous system regions for ATP-dependent interleukin-1beta release. Sci. Rep 4, 6824 10.1038/srep06824 [PubMed: 25351234]

Field R, Campion S, Warren C, Murray C, Cunningham C, 2010 Systemic challenge with the TLR3 agonist poly I:C induces amplified IFNalpha/beta and IL-1beta responses in the diseased brain and exacerbates chronic neurodegeneration. Brain. Behav. Immun 24, 996–1007. 10.1016/j.bbi.2010.04.004 [PubMed: 20399848]

Garcia-Cattaneo A, Gobert F-X, Muller M, Toscano F, Flores M, Lescure A, Del Nery E, Benaroch P, 2012 Cleavage of Toll-like receptor 3 by cathepsins B and H is essential for signaling. Proc. Natl. Acad. Sci. U. S. A 109, 9053–9058. 10.1073/pnas.1115091109 [PubMed: 22611194]

Hixson JE, Vernier DT, 1990 Restriction isotyping of human apolipoprotein E by gene amplification and cleavage with HhaI. J. Lipid Res 31, 545–548. [PubMed: 2341813]

Jack CS, Arbour N, Blain M, Meier U-C, Prat A, Antel JP, 2007 Th1 polarization of CD4+ T cells by Toll-like receptor 3-activated human microglia. J. Neuropathol. Exp. Neurol 66, 848–859. 10.1097/nen.0b013e3181492a7 [PubMed: 17805015]

Jackson AC, Rossiter JP, Lafon M, 2006 Expression of Toll-like receptor 3 in the human cerebellar cortex in rabies, herpes simplex encephalitis, and other neurological diseases. J. Neurovirol 12, 229–234. 10.1080/13550280600848399 [PubMed: 16877304]

Jeong S-Y, Jeon R, Choi YK, Jung JE, Liang A, Xing C, Wang X, Lo EH, Song YS, 2015 Activation of microglial TLR3 promotes neuronal survival against cerebral ischemia. J. Neurochem 10.1111/jnc.13441

Kariko K, Bhuyan P, Capodici J, Weissman D, 2004a Small interfering RNAs mediate sequence-independent gene suppression and induce immune activation by signaling through toll-like receptor 3. J. Immunol 172, 6545–6549. [PubMed: 15153468]

Kariko K, Ni H, Capodici J, Lamphier M, Weissman D, 2004b mRNA is an endogenous ligand for Toll-like receptor 3. J. Biol. Chem 279, 12542–12550. 10.1074/jbc.M310175200 [PubMed: 14729660]

Kawai T, Akira S, 2007a. Signaling to NF-kappaB by Toll-like receptors. Trends Mol. Med 13, 460–469. 10.1016/j.molmed.2007.09.002 [PubMed: 18029230]

Kawai T, Akira S, 2007b TLR signaling. Semin. Immunol 19, 24–32. 10.1016/j.smim.2006.12.004 [PubMed: 17275323]

Kim C, Lee H-J, Masliah E, Lee S-J, 2016 Non-cell-autonomous Neurotoxicity of alpha-synuclein Through Microglial Toll-like Receptor 2. Exp. Neurobiol 25, 113–119. 10.5607/en.2016.25.3.113 [PubMed: 27358579]

Krstic D, Madhusudan A, Doehner J, Vogel P, Notter T, Imhof C, Manalastas A, Hilfiker M, Pfister S, Schwerdel C, Riether C, Meyer U, Knuesel I, 2012 Systemic immune challenges trigger and drive Alzheimer-like neuropathology in mice. J. Neuroinflammation 9, 151 10.1186/1742-2094-9-151 [PubMed: 22747753]

Lathia JD, Okun E, Tang S-C, Griffioen K, Cheng A, Mughal MR, Laryea G, Selvaraj PK, ffrench-Constant C, Magnus T, Arumugam TV, Mattson MP, 2008 Toll-like receptor 3 is a negative regulator of embryonic neural progenitor cell proliferation. J. Neurosci 28, 13978–13984. 10.1523/JNEUROSCI.2140-08.2008 [PubMed: 19091986]

Leifer CA, Medvedev AE, 2016 Molecular mechanisms of regulation of Toll-like receptor signaling. J. Leukoc. Biol 100, 927–941. 10.1189/jlb.2MR0316-117RR [PubMed: 27343013]

Li J, Wang Y, Wang X, Ye L, Zhou Y, Persidsky Y, Ho W, 2013 Immune activation of human brain microvascular endothelial cells inhibits HIV replication in macrophages. Blood 121, 2934–2942. 10.1182/blood-2012-08-450353 [PubMed: 23401273]

Li Y, Xu X-L, Zhao D, Pan L-N, Huang C-W, Guo L-J, Lu Q, Wang J, 2015 TLR3 ligand Poly IC Attenuates Reactive Astrogliosis and Improves Recovery of Rats after Focal Cerebral Ischemia. CNS Neurosci. Ther 21, 905–913. 10.1111/cns.12469 [PubMed: 26494128]

Majde JA, Kapas L, Bohnet SG, De A, Krueger JM, 2010 Attenuation of the influenza virus sickness behavior in mice deficient in Toll-like receptor 3. Brain. Behav. Immun 24, 306–315. 10.1016/j.bbi.2009.10.011 [PubMed: 19861156]

Mastroeni D, Nolz J, Sekar S, Delvaux E, Serrano G, Cuyugan L, Liang WS, Beach TG, Rogers J, Coleman PD, 2018 Laser-captured microglia in the Alzheimer's and Parkinson's brain reveal unique regional expression profiles and suggest a potential role for hepatitis B in the Alzheimer's brain. Neurobiol. Aging 63, 12–21. 10.1016/j.neurobiolaging.2017.10.019 [PubMed: 29207277]

McKeith IG, Dickson DW, Lowe J, Emre M, O'Brien JT, Feldman H, Cummings J, Duda JE, Lippa C, Perry EK, Aarsland D, Arai H, Ballard CG, Boeve B, Burn DJ, Costa D, Del Ser T, Dubois B, Galasko D, Gauthier S, Goetz CG, Gomez-Tortosa E, Halliday G, Hansen LA, Hardy J, Iwatsubo T, Kalaria RN, Kaufer D, Kenny RA, Korczyn A, Kosaka K, Lee VMY, Lees A, Litvan I, Londos E, Lopez OL, Minoshima S, Mizuno Y, Molina JA, Mukaetova-Ladinska EB, Pasquier F, Perry RH, Schulz JB, Trojanowski JQ, Yamada M, 2005 Diagnosis and management of dementia with Lewy bodies: third report of the DLB Consortium. Neurology 65, 1863–72. 10.1212/01.wnl.0000187889.17253.b1 [PubMed: 16237129]

Muzio M, Bosisio D, Polentarutti N, D'amico G, Stoppacciaro A, Mancinelli R, van't Veer C, Penton-Rol G, Ruco LP, Allavena P, Mantovani A, 2000 Differential expression and regulation of toll-like receptors (TLR) in human leukocytes: selective expression of TLR3 in dendritic cells. J. Immunol 164, 5998–6004. [PubMed: 10820283]

Nagyoszi P, Wilhelm I, Farkas AE, Fazakas C, Dung NTK, Hasko J, Krizbai IA, 2010 Expression and regulation of toll-like receptors in cerebral endothelial cells. Neurochem. Int 57, 556–564. 10.1016/j.neuint.2010.07.002 [PubMed: 20637248]

Nazmi A, Dutta K, Hazra B, Basu A, 2014 Role of pattern recognition receptors in flavivirus infections. Virus Res. 185, 32–40. 10.1016/j.virusres.2014.03.013 [PubMed: 24657789]

Newell KL, Hyman BT, Growdon JH, Hedley-Whyte ET, 1999 Application of the National Institute on Aging (NIA)-Reagan Institute criteria for the neuropathological diagnosis of Alzheimer disease. J. Neuropathol. Exp. Neurol 58, 1147–1155. [PubMed: 10560657]

O'Neill LAJ, Golenbock D, Bowie AG, 2013 The history of Toll-like receptors - redefining innate immunity. Nat. Rev. Immunol 10.1038/nri3446

Okun E, Griffioen K, Barak B, Roberts NJ, Castro K, Pita MA, Cheng A, Mughal MR, Wan R, Ashery U, Mattson MP, 2010 Toll-like receptor 3 inhibits memory retention and constrains adult hippocampal neurogenesis. Proc. Natl. Acad. Sci. U. S. A 107, 15625–15630. 10.1073/pnas.1005807107 [PubMed: 20713712]

Pan L, Zhu W, Li C, Xu X, Guo L, Lu Q, 2012 Toll-like receptor 3 agonist Poly I:C protects against simulated cerebral ischemia in vitro and in vivo. Acta Pharmacol. Sin 33, 1246–1253. 10.1038/aps.2012.122 [PubMed: 22983393]

Readhead B, Haure-Mirande J-V, Funk CC, Richards MA, Shannon P, Haroutunian V, Sano M, Liang WS, Beckman ND, Price ND, Reiman EM, Schadt EE, Ehrlich ME, Gandy S, Dudley JT, 2018 Multiscale Analysis of Independent Alzheimer's Cohorts Finds Disruption of Molecular, Genetic, and Clinical Networks by Human Herpesvirus. Neuron

Reed-Geaghan EG, Savage JC, Hise AG, Landreth GE, 2009. CD14 and toll-like receptors 2 and 4 are required for fibrillar A{beta}-stimulated microglial activation. J. Neurosci 29, 11982–11992. 10.1523/JNEUROSCI.3158-09.2009 [PubMed: 19776284]

Scholtzova H, Chianchiano P, Pan J, Sun Y, Goni F, Mehta PD, Wisniewski T, 2014 Amyloid beta and Tau Alzheimer's disease related pathology is reduced by Tolllike receptor 9 stimulation. Acta Neuropathol. Commun 2, 101 10.1186/s40478-014-0101-2 [PubMed: 25178404]

Scholtzova H, Do E, Dhakal S, Sun Y, Liu S, Mehta PD, Wisniewski T, 2017 Innate Immunity Stimulation via Toll-Like Receptor 9 Ameliorates Vascular Amyloid Pathology in Tg-SwDI Mice with Associated Cognitive Benefits. J. Neurosci 37, 936–959. 10.1523/JNEUROSCI.1967-16.2016 [PubMed: 28123027]

Scholtzova H, Kascsak RJ, Bates KA, Boutajangout A, Kerr DJ, Meeker HC, Mehta PD, Spinner DS, Wisniewski T, 2009 Induction of toll-like receptor 9 signaling as a method for ameliorating Alzheimer's disease-related pathology. J. Neurosci. 29, 1846–1854. 10.1523/JNEUROSCI.5715-08.2009 [PubMed: 19211891]

Shi H, Gabarin N, Hickey E, Askalan R, 2013 TLR-3 receptor activation protects the very immature brain from ischemic injury. J. Neuroinflammation 10, 104 10.1186/1742-2094-10-104 [PubMed: 23965176]

Su F, Bai F, Zhou H, Zhang Z, 2016 Microglial toll-like receptors and Alzheimer's disease. Brain. Behav. Immun 52, 187–198. 10.1016/j.bbi.2015.10.010 [PubMed: 26526648]

Takeuchi O, Hemmi H, Akira S, 2004 Interferon response induced by Toll-like receptor signaling. J. Endotoxin Res 10, 252–256. 10.1179/096805104225005896 [PubMed: 15373970]

Tarassishin L, Suh H-S, Lee SC, 2011 Interferon regulatory factor 3 plays an antiinflammatory role in microglia by activating the PI3K/Akt pathway. J. Neuroinflammation 8, 187 10.1186/1742-2094-8-187 [PubMed: 22208359]

Toscano F, Estornes Y, Virard F, Garcia-Cattaneo A, Pierrot A, Vanbervliet B, Bonnin M, Ciancanelli MJ, Zhang S-Y, Funami K, Seya T, Matsumoto M, Pin J-J, Casanova J-L, Renno T, Lebecque S, 2013 Cleaved/associated TLR3 represents the primary form of the signaling receptor. J. Immunol 190, 764–773. 10.4049/jimmunol.1202173 [PubMed: 23255358]

Vidya MK, Kumar VG, Sejian V, Bagath M, Krishnan G, Bhatta R, 2017 Toll-like receptors: Significance, ligands, signaling pathways, and functions in mammals. Int. Rev. Immunol 1–17. 10.1080/08830185.2017.1380200 [PubMed: 28215101]

Vontell R, Supramaniam V, Thornton C, Wyatt-Ashmead J, Mallard C, Gressens P, Rutherford M, Hagberg H, 2013 Toll-like receptor 3 expression in glia and neurons alters in response to white matter injury in preterm infants. Dev. Neurosci 35, 130–139. 10.1159/000346158 [PubMed: 23548575]

Vontell R, Supramaniam V, Wyatt-Ashmead J, Gressens P, Rutherford M, Hagberg H, Thornton C, 2015 Cellular mechanisms of toll-like receptor-3 activation in the thalamus are associated with white matter injury in the developing brain. J. Neuropathol. Exp. Neurol 74, 273–285. 10.1097/NEN.0000000000000172 [PubMed: 25668563]

Walker DG, Dalsing-Hernandez JE, Campbell NA, Lue L-F, 2009 Decreased expression of CD200 and CD200 receptor in Alzheimer's disease: a potential mechanism leading to chronic inflammation. Exp. Neurol 215, 5–19. 10.1016/j.expneurol.2008.09.003 [PubMed: 18938162]

Walker DG, Link J, Lue L-F, Dalsing-Hernandez JE, Boyes BE, 2006 Gene expression changes by amyloid beta peptide-stimulated human postmortem brain microglia identify activation of multiple inflammatory processes. J. Leukoc. Biol 79, 596–610. 10.1189/jlb.0705377 [PubMed: 16365156]

Walker DG, Whetzel AM, Lue L-F, 2015 Expression of suppressor of cytokine signaling genes in human elderly and Alzheimer's disease brains and human microglia. Neuroscience 302, 121–37. 10.1016/j.neuroscience.2014.09.052 [PubMed: 25286386]

Walker DG, Whetzel AM, Serrano G, Sue LI, Beach TG, Lue L-F, 2015 Association of CD33 polymorphism rs3865444 with Alzheimer's disease pathology and CD33 expression in human

cerebral cortex. Neurobiol. Aging 36, 571–82. 10.1016/j.neurobiolaging.2014.09.023 [PubMed: 25448602]

Wang P-F, Fang H, Chen J, Lin S, Liu Y, Xiong X-Y, Wang Y-C, Xiong R-P, Lv F-L, Wang J, Yang Q-W, 2014 Polyinosinic-polycytidylic acid has therapeutic effects against cerebral ischemia/reperfusion injury through the downregulation of TLR4 signaling via TLR3. J. Immunol 192, 4783–4794. 10.4049/jimmunol.1303108 [PubMed: 24729619]

Wang T, Town T, Alexopoulou L, Anderson JF, Fikrig E, Flavell RA, 2004 Toll-like receptor 3 mediates West Nile virus entry into the brain causing lethal encephalitis. Nat. Med 10, 1366–1373. 10.1038/nm1140 [PubMed: 15558055]

Xu Y, Liu X-D, Gong X, Eissa NT, 2008 Signaling pathway of autophagy associated with innate immunity. Autophagy 4, 110–112. [PubMed: 18059159]

Zhan Z, Xie X, Cao H, Zhou X, Zhang XD, Fan H, Liu Z, 2014 Autophagy facilitates TLR4- and TLR3-triggered migration and invasion of lung cancer cells through the promotion of TRAF6 ubiquitination. Autophagy 10, 257–268. 10.4161/auto.27162 [PubMed: 24321786]

Zhou J, Zhou N, Wu X-N, Cao H-J, Sun Y-J, Zhang T-Z, Chen K-Y, Yu D-M, 2015 Role of the Tolllike receptor 3 signaling pathway in the neuroprotective effect of sevoflurane preconditioning during cardiopulmonary bypass in rats. Mol. Med. Rep 12, 7859–7868. 10.3892/mmr.2015.4420 [PubMed: 26460219]

Highlights

- Increased TLR-3 immunoreactivity and mRNA in middle temporal gyrus oAlzheimer's disease cases
- TLR-3 was localized to most microglia and strongest in microglia associated with amyloid plaques
- Microglia TLR-3 immunoreactivity colocalized with endosomal/lysosomal marker CD68
- TLR-3, IRF-3 and TLR-9 mRNA expression positively correlated with AD plaque and tangle pathology
- Treatment of cultured human microglia with Aβ 1–42 did not increase expression of TLR-3

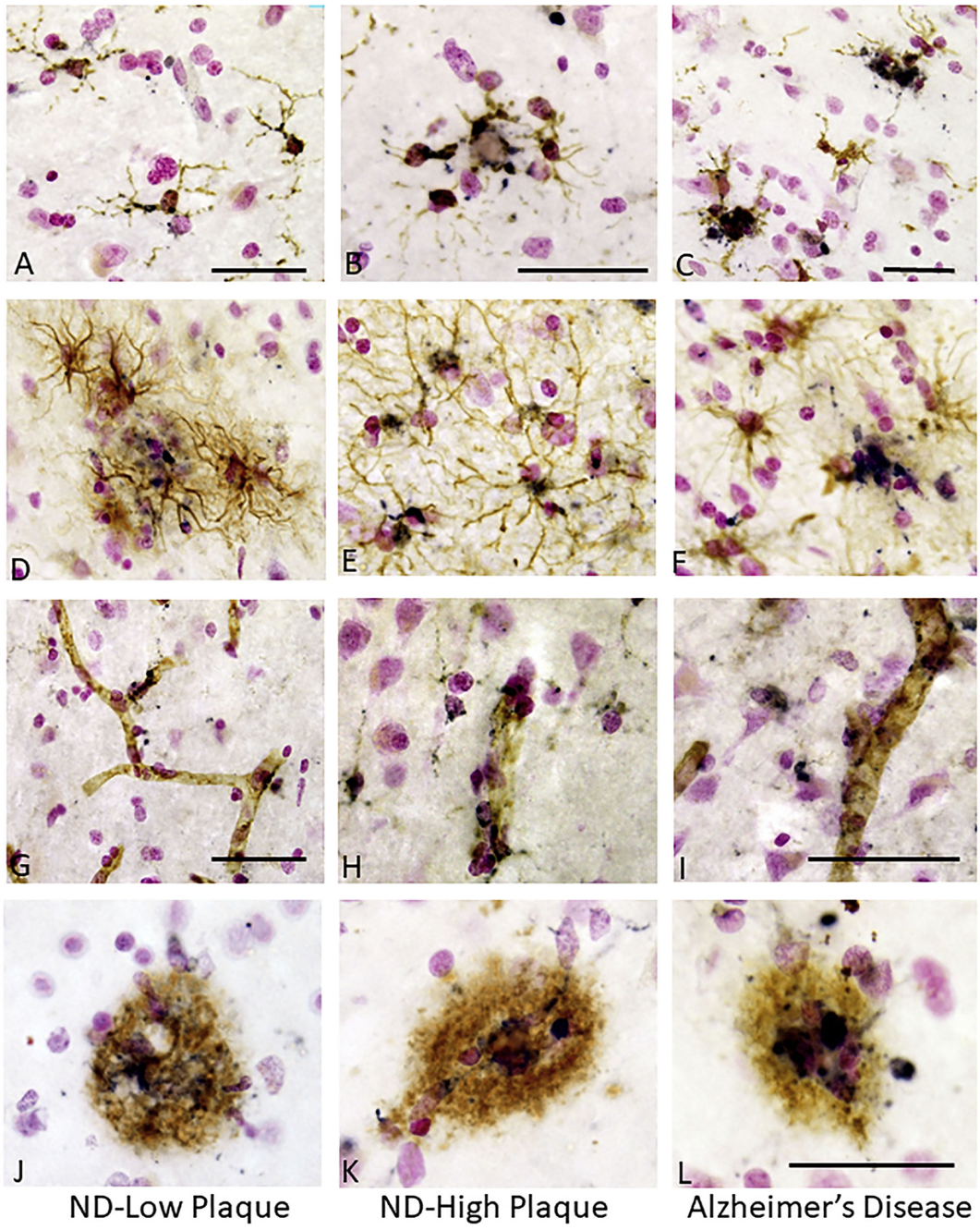

Figure 1. Identification of TLR-3 immunoreactive microglia, astrocytes, endothelial cells and plaques in human middle temporal gyrus.

A – C. TLR-3 immunoreactivity in microglia. Sections from non-demented (ND) – low plaque (A), ND high plaque (B) and Alzheimer's disease (C) cases. Sections were double stained with antibody to TLR-3 (purple) and IBA-1 (brown). TLR-3 immunoreactivity was present in microglia with different intensities, even in microglia in NDLP cases. These microglia had the morphology of non-activated cells. Panels B and C show stronger immunoreactivity. Bars represent 50μm.

D – F. TLR-3 immunoreactivity in astrocytes. TLR-3 expression in astrocytes was not an abundant feature. Sections from ND – low plaque (**D**), ND-high plaque (**E**) and Alzheimer's disease (**F**) cases. Sections were double stained with antibody to TLR-3 (purple) and GFAP (brown) to identify astrocytes.

G – H. TLR-3 immunoreactivity in vascular endothelial cells. Sections from ND – low plaque (**G**), ND- high plaque (**H**) and Alzheimer's disease (**I**) cases. Sections were double stained with antibody to TLR-3 (purple) and CD31 (brown) to identify endothelial cells. TLR-3 immunoreactivity was present in vascular endothelial cells in all disease groups. Bars represent 50 μm.

J - L. TLR-3 immunoreactivity colocalization with Aβ positive plaques. Sections from ND – low plaque (J), ND-high plaque (K) and Alzheimer's disease (L) cases. Sections were double stained with antibody to TLR-3 (purple) and 6E10 (brown) to identify Aβ peptide. Immunoreactive cells colocalized with most Aβ plaques even on the few plaques present in the ND-low plaque cases (panel J). Stronger staining is evident on plaques in AD cases (K). Bars represent 50 μm.

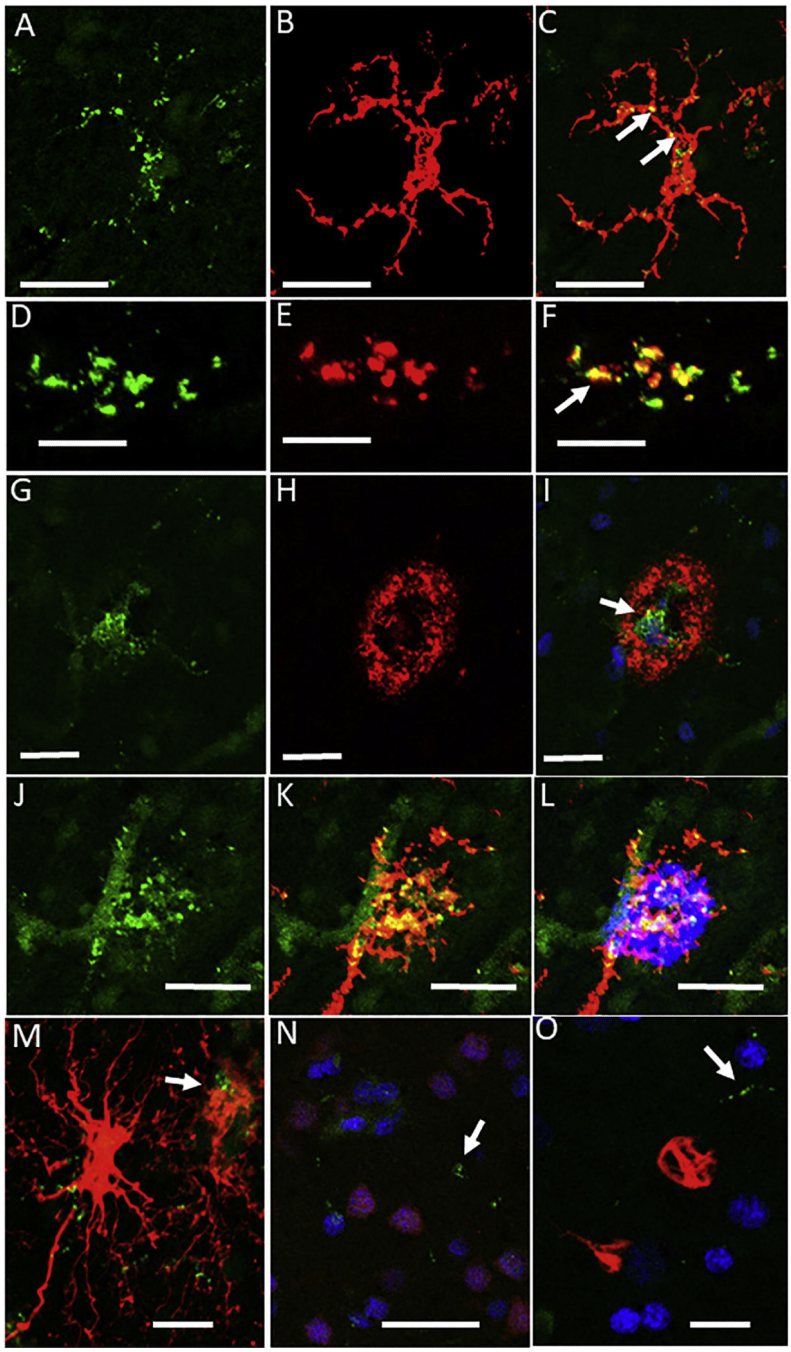

Figure 2. Features of TLR-3 immunohistochemistry in AD brains

Confocal microscopy was carried out to validate TLR-3 localization patterns. All staining illustrated were from AD cases as these had stronger TLR-3 immunoreactivity.

A-C. Colocalization of TLR-3 (green-**A**) with microglia stained with IBA-1 (red –**B**). Merged images show TLR-3 positive structures (yellow-**C**) within microglia cell. Scale bars indicate 40 μm

D-F. Colocalization of TLR-3 (green-**D**) with microglia stained with CD68 (red –**E**). Merged images show that most TLR-3 positive structures colocalize (arrows yellow –**F**) with this

phagocytic cell-associated lysosome protein, but this is not complete (distinct green and red in merged image)(**F**) within microglia cell. Scale bars indicate 10 μm.

G-I. Colocalization of TLR-3 (green-**G**) with Aβ plaque identified with antibody 6E10 (red –**H**). Merged images show limited TLR-3 positive structures (arrows yellow-I) within center of Aβ plaque. There is limited yellow staining. This shows that most Aβ does not become localized to TLR-3 positive structures. DAPI counterstaining identifies nuclei. Scale bars indicate 20 μm.

J-L. Colocalization of TLR-3, IBA-1 and Aβ. This image confirms that the strongest TLR-3 (green-J) positive microglia (IBA-1, red-**K**) are colocalized (yellow) on plaques (blue –**L**). TLR-3 positive endothelial cells (arrowhead) (green –**G**) can be observed separate from microglia. Scale bars indicate 25 μm.

M. Limited colocalization of TLR-3 with GFAP positive astrocytes (arrow). Most strongly staining GFAP astrocytes do not contain TLR-3 positive structures. Scale bars indicate 20 μm.

N. Absence of colocalization of TLR-3 (green) with NeuN positive neurons (Purple). This image discriminates between NeuN positive DAPI-stained nuclei (purple) and other cell type DAPI stained nuclei (blue). TLR-3 immunoreactivity (green) is not associated with NeuN positive structures. Scale bars indicate 50 μm.

L. Absence of colocalization of TLR-3 (green) with the autophagy/ubiquitn receptor protein p62 (red) that is staining subsets of neurofibrillary tangles. Scale bars indicate 20 μm.

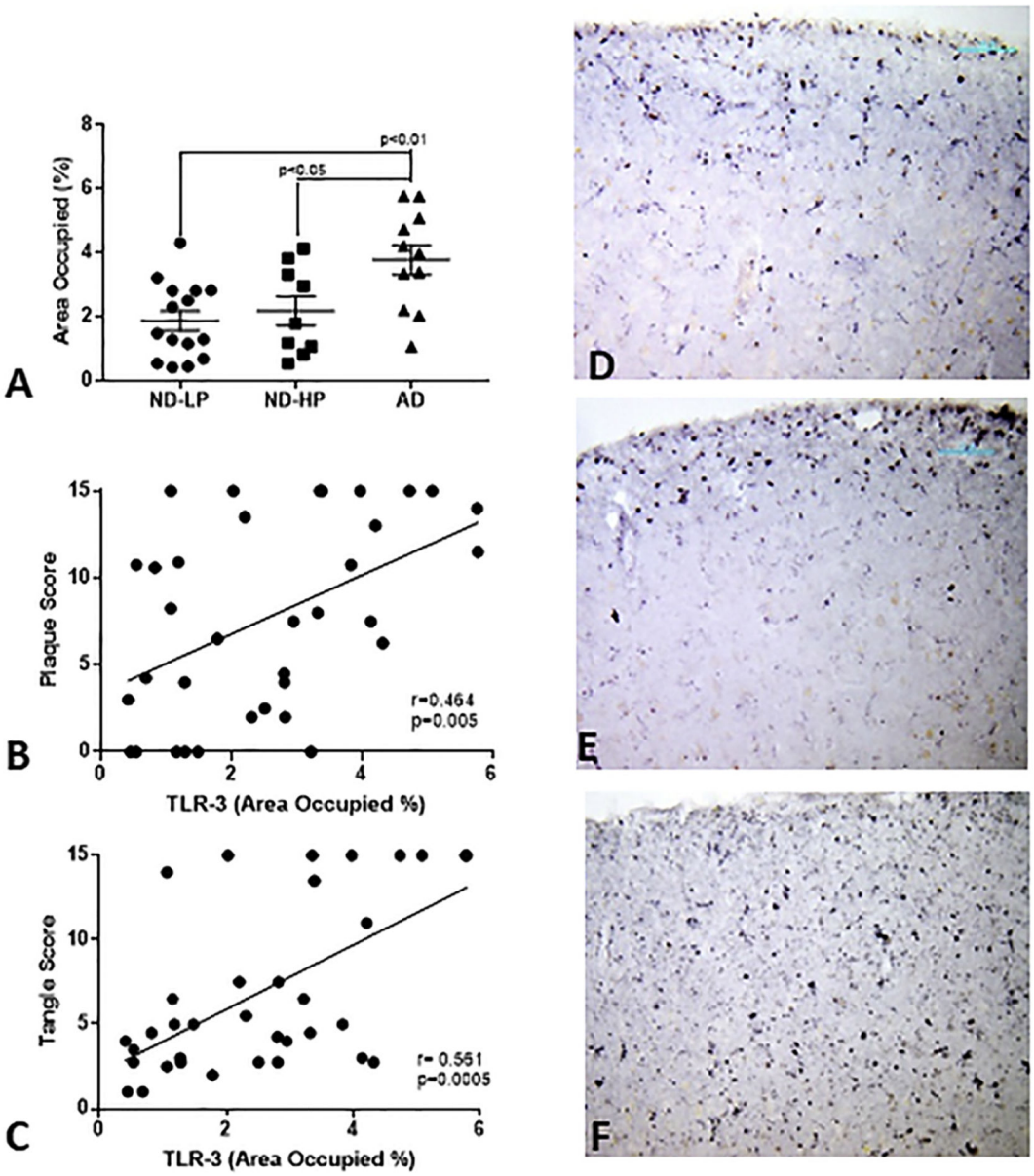

Figure 3. Quantitative Analysis of TLR-3 immunoreactivity in middle temporal gyrus.

Sections from non-demented – low plaque (ND-LP)(n= 15), non-demented high plaque (ND-HP) (n= 10) and Alzheimer's disease (AD)(n=11) cases were single stained for TLR-3 under matching conditions. For each section, 4 separate low-power (4x) pictures were collected across cortical layers and analyzed for area of immunoreactivity using Image J software. Significant increase in mean area of immunoreactivity was detected in AD cases (A). Amounts of TLR-3 immunoreactivity positively correlated with overall plaque (B) and tangle scores (C) for these cases. Representative low-magnification images of TLR-3 immunoreactivity for ND-LP (D), ND-HP (E) and AD (F) cases are shown.

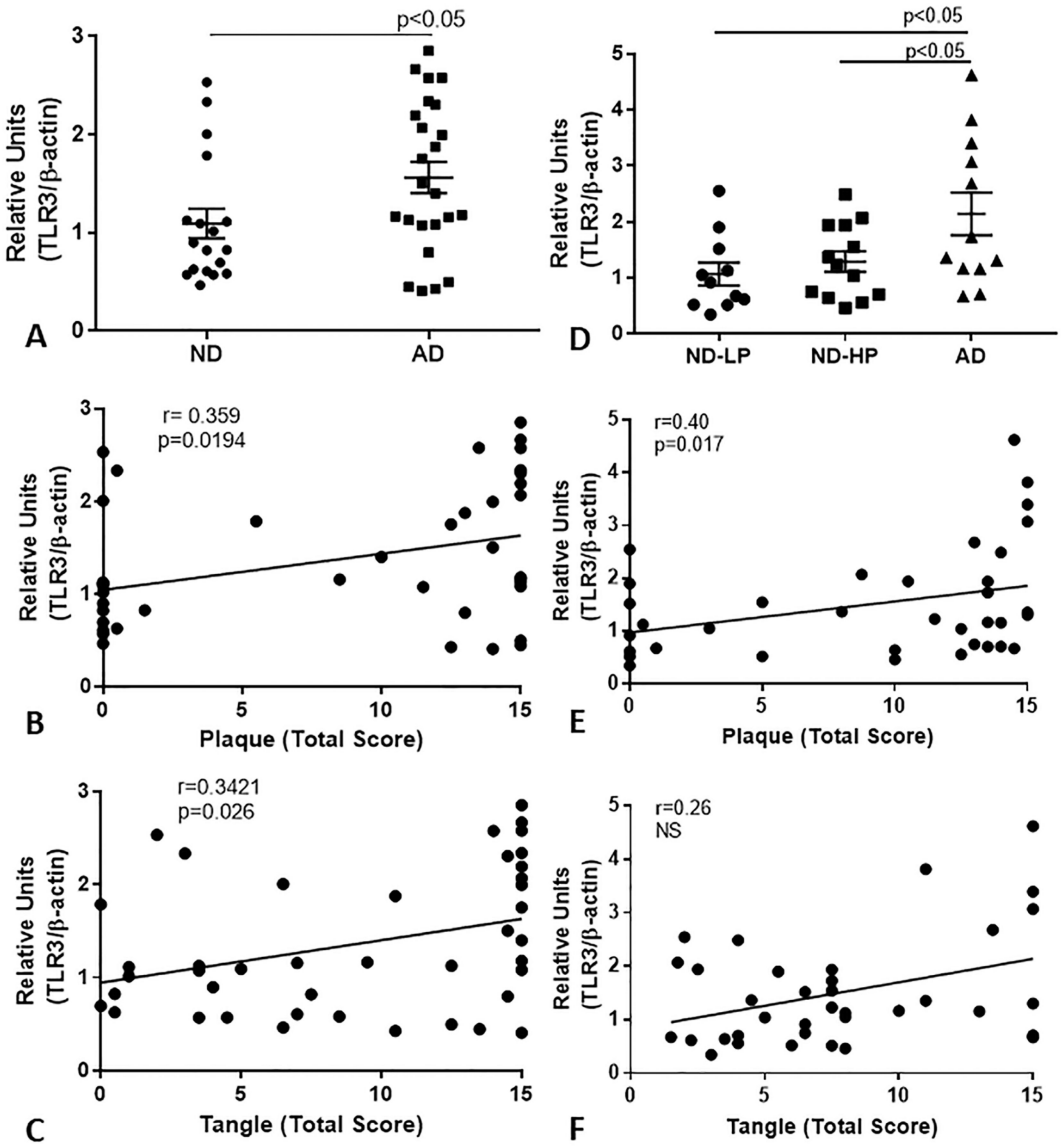

Figure 4. Expression levels of TLR-3 mRNA in two series of AD and non-demented brain samples.

Quantitative real time reverse transcription-polymerase chain reaction (qPCR) analyses of TLR-3 mRNA expression in middle temporal gyrus of series of low plaque ND cases (n=18) and AD cases (n=24) (A) and a series of ND-LP (n=11), ND-HP (n=13) and AD cases (n=12) (D) demonstrate significant increase in TLR-3 mRNA in AD cases. Correlation analyses of TLR-3 mRNA values from both series with corresponding plaque and tangle ranking scores showed significant correlation with plaque scores (B and D) and tangle scores for first series (C), but not for second series of brain samples.

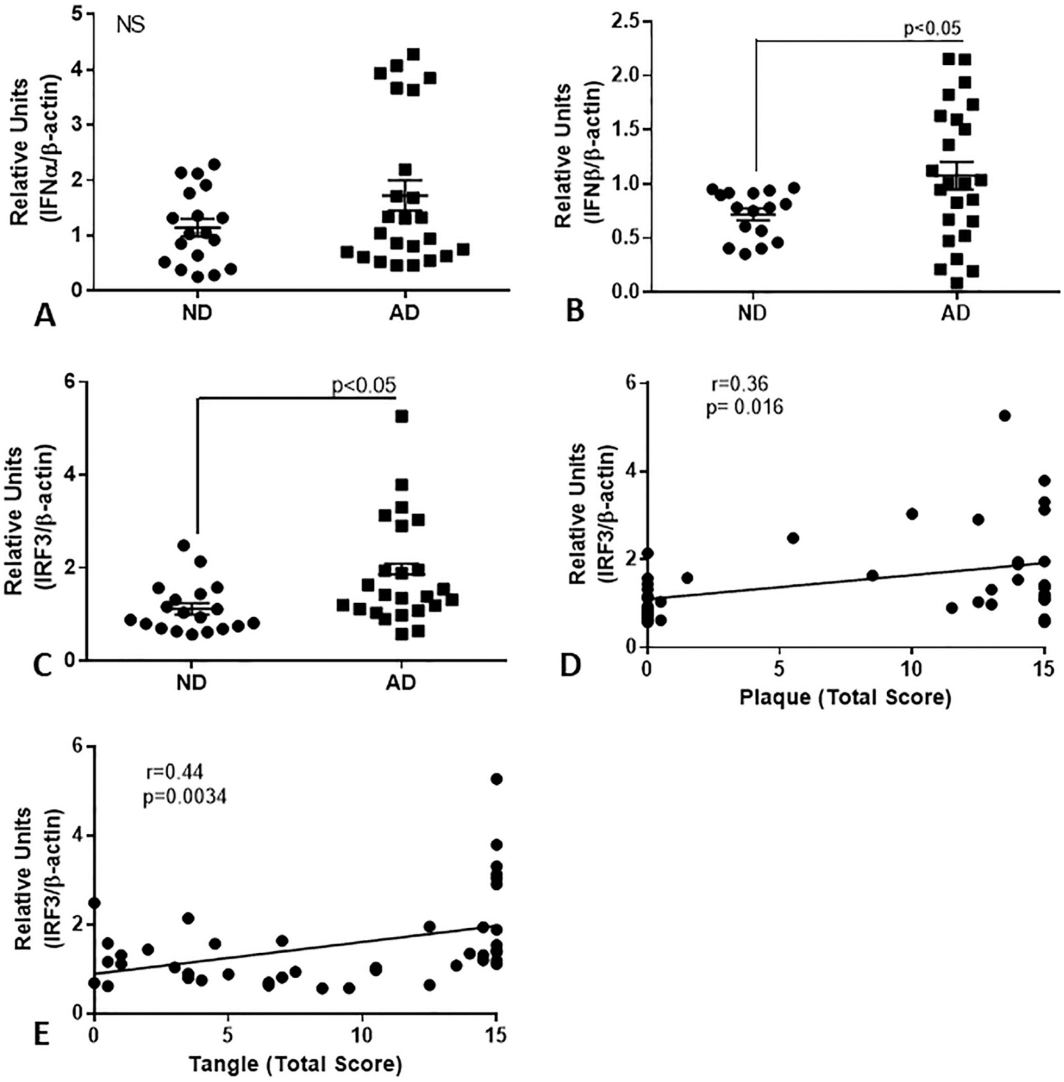

Figure 5. Expression of TLR-3-associated signaling genes in series of AD and nondemented brain samples.

QPCR analyses of expression of interferon alpha (IFN-α) (A), interferon beta (IFN-β)(B) and interferon regulatory factor (IRF)-3 (C) in middle temporal gyrus of series of low plaque ND cases (n=18) and AD cases (n=24) of low plaque ND cases (n=18) and AD cases (n=24). There was significantly increased expression of IFN-β and IRF-3, but not IFN-α in the AD cases. Expression levels of IRF-3 correlated weakly with plaque score (D)(Spearman r = 0.381, p=0.012) and strongly with tangle scores (E) for these cases (r=0.413, p=0.0059).

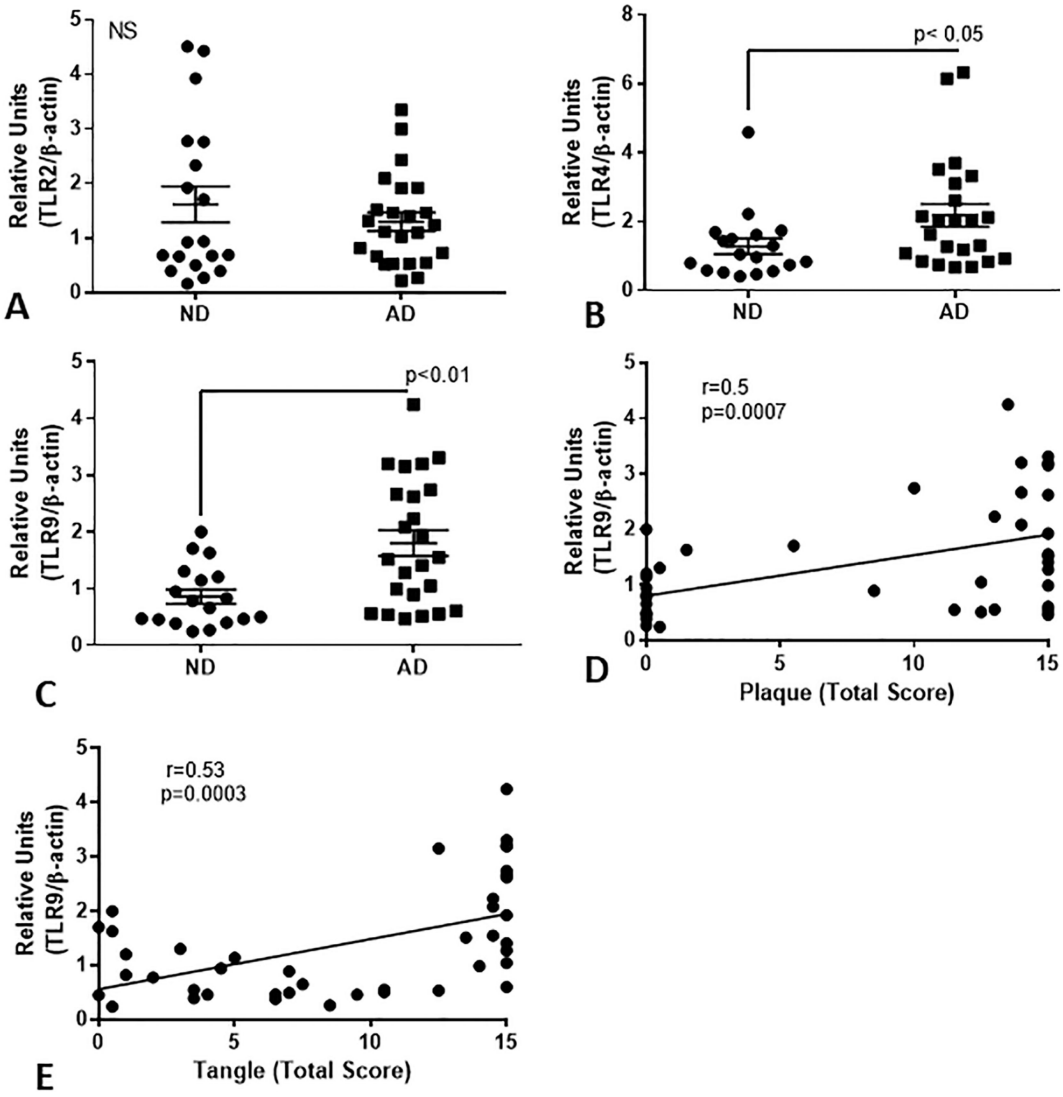

Figure 6. Expression of AD-associated TLR genes TLR-2, TLR-4 and TLR-9 in series of AD and non-demented brain samples.

QPCR analyses of expression of TLR-2 (**A**), TLR-4 (**B**) and TLR-9 (**C**) in middle temporal gyrus of series of low plaque ND cases (n=18) and AD cases (n=24) of low plaque ND cases (n=18) and AD cases (n=24). There was significantly increased expression of TLR-4 and TLR-9, but not TLR-2 in the AD cases. Expression levels of TLR-9 correlated with plaque score (Spearman r = 0.4936, p=0.0009) (**D**) and with tangle scores for these cases (r=0.515, p=0.0005).

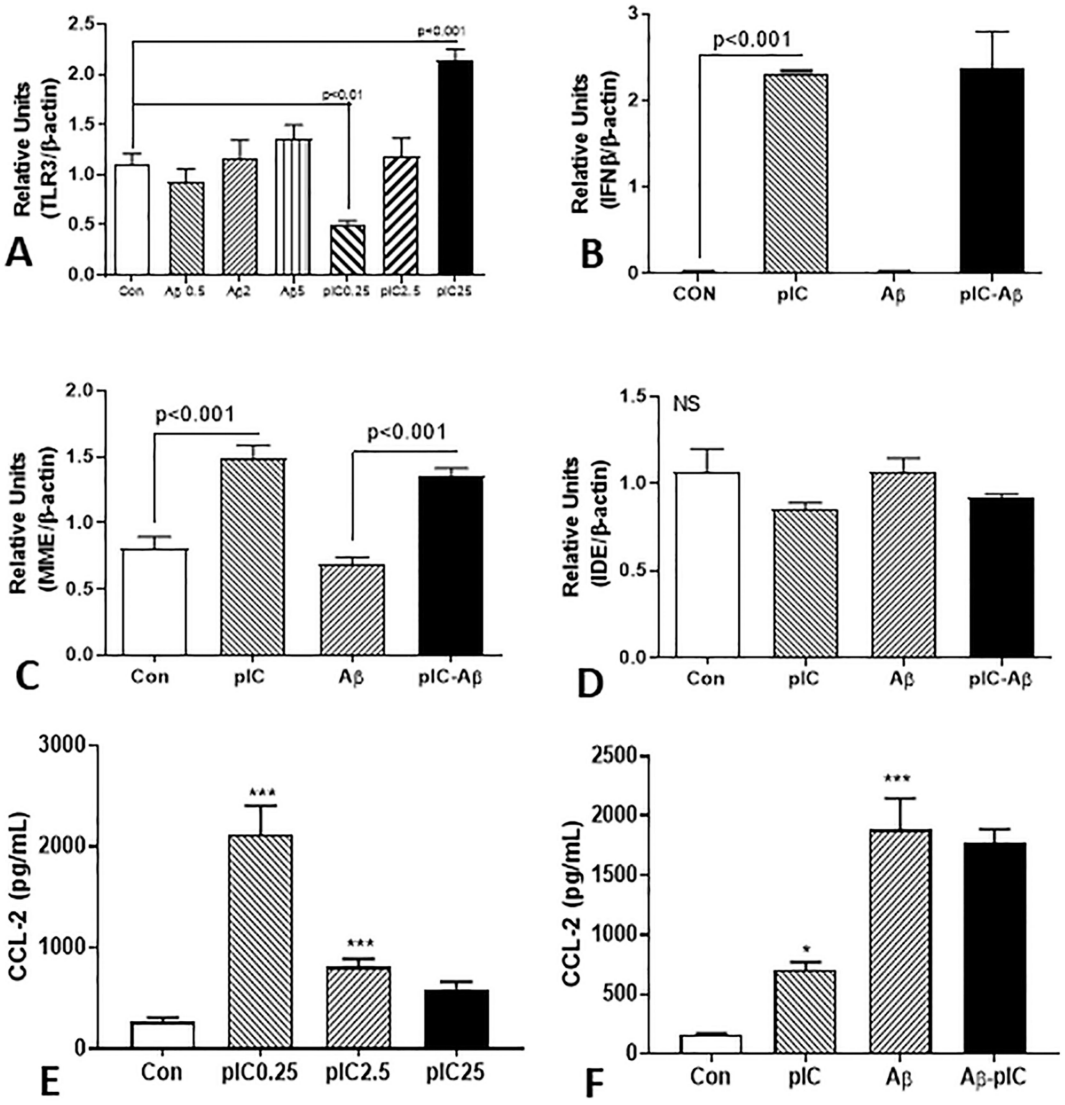

Figure 7. Interaction of Aβ and TLR-3 stimulating ligand poly I:C on stimulation of human brain microglia.

(A). Real time PCR analyses showing effects of different Aβ and poly IC doses on stimulation of TLR-3 expression. Results show that Aβ doses did not significantly change TLR-3 mRNA expression in microglia (n=3), while different doses of poly I:C (pIC) had biphasic response. Low dose 0.25 μg/ml (PIC 0.25) significantly inhibited TLR-3 expression ($p<0.01$), middle dose (2.5 μg/ml) had no significant effect while highest dose (25 μg/ml) had significant stimulation.

B). Stimulation of IFN-β mRNA expression by poly I:C (2.5 μg/ml) was not modulated by Aβ (2 μM). Results show strong induction of IFN-β mRNA expression by poly I:C (2.5 μg/ml dose) in human microglia. There was no induction with Aβ (1 μM) treatment. Aβ treatment did not modulate effects of poly I:C.

(C and D). Poly I:C treatment of microglia stimulated expression of Aβ degrading enzyme neprilysin (MME) mRNA but not insulin degrading enzyme (IDE). Results show induction of neprilysin (MME) mRNA expression by poly I:C (2.5μg/ml dose) in

human microglia, but there was no induction with Aβ (1 μM) treatment (**D**). Aβ treatment did not modulate effects of poly I:C. Poly I:C or Aβ did not significantly affect expression of insulin degrading enzyme (IDE).

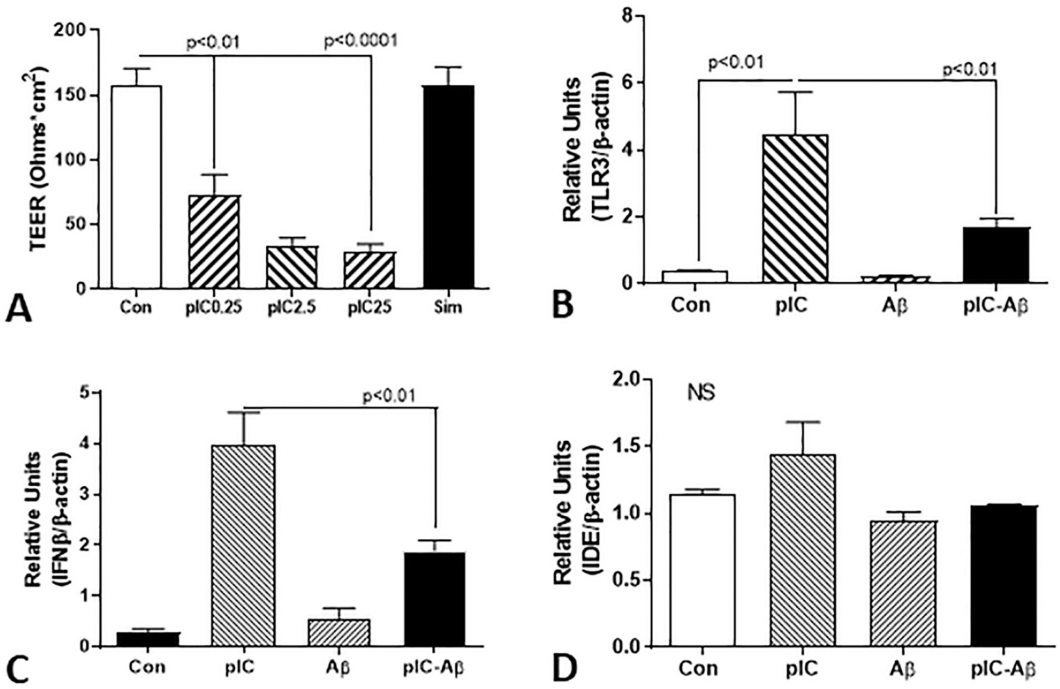

Figure 8. Interaction of Aβ and TLR-3 stimulating ligand poly I:C on human brain endothelial cells

(A) Poly I:C treatment of brain endothelial cells resulted in significant dose dependent reduction of transendothelial electrical resistance (TEER). An *in vitro* model of blood brain barrier (BBB) with BEC grown on semi-permeable inserts involving measurement of TEER to indicate tightness of interaction of cells. BEC cells treated with different doses of poly I:C (pIC) showed significant reduction of TEER indicating weakening of cellular interactions. As a control, cells treated with simvastatin (20 μM) maintained TEER values. Results show mean ± S.E.M: ** $p<0.01$, **** $p<0.0001$.

(B). Real time PCR analyses showing effects of Aβ and poly I:C on stimulation of TLR-3 expression by brain endothelial cells. Unlike microglia, poly I:C (pIC) stimulation of BEC (2.5 μg/ml) resulted in significant increased expression of TLR-3. Treatment of HBEC with poly I:C and Aβ resulted in significant inhibition of TLR-3 induction. Results show mean ± S.E.M: ** $p<0.01$.

(C). Real time PCR analyses showing effects of Aβ and poly I:C on stimulation of IFN-β expression by brain endothelial cells. Poly I:C stimulation of HBEC (2.5 μg/ml) resulted in significant increased expression of IFN-β mRNA. Treatment of BEC with poly I:C and Aβ resulted in significant inhibition of IFN-β induction. Results show mean ± S.E.M: ** $p<0.01$.

(D). Real time PCR analyses showing absence of effects of Aβ and poly I:C on insulin degrading enzyme expression by brain endothelial cells. PIC stimulation of HBEC (2.5 μg/ml) resulted in non-significant increase in expression of IDE mRNA. Treatment of BEC with pIC and Aβ had no significant effect. Results show mean ± S.E.M.

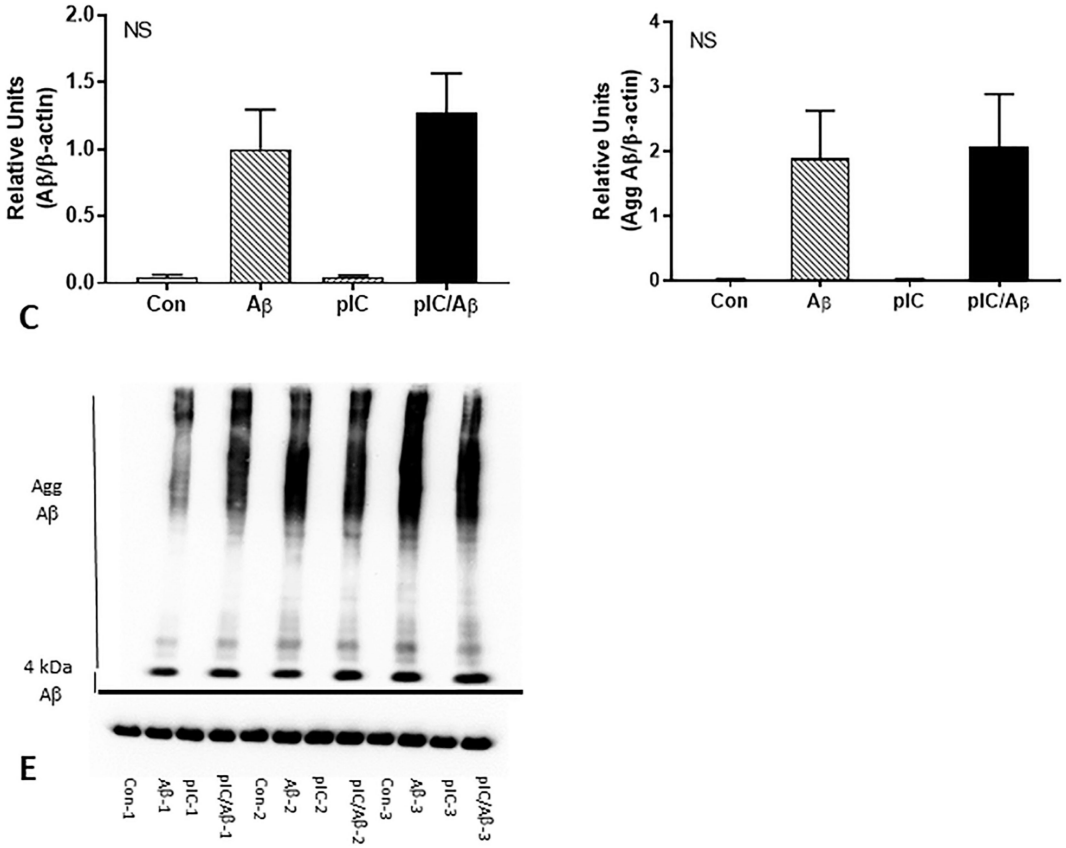

Figure 9. Effects on TLR-3 stimulating ligand poly I:C on human brain microglia activation and Aβ degradation.

(A and B). Differential effects of poly I:C and Aβ on stimulation of chemokine CCL2 by human microglia.

(**A**). Low dose of poly I:C (pIC) (0.25 μg/ml) stimulated microglia secretion of CCL2 at higher levels than poly I:C (2.5 μg/ml and 25 μg/ml) doses. Media assayed using ELISA. Results show mean ± S.E.M: * $p<0.05$, ** $p<0.01$, *** $p<0.001$ compared to control unstimulated values.

(**B**). Aβ stimulated increase in secretion of CCL2 not modulated by co-treatment with poly I:C. Microglia were stimulated with poly I:C (2.5 μg/ml), Aβ 2 μM or combination of both for 24 hours. Media were collected and assay by ELISA. Results show mean ± S.E.M: * $p<0.05$, *** $p<0.001$ compared to control unstimulated values.

(C – E) Co-treatment of Aβ stimulated microglia with poly I:C did not alter Aβ degradation. Western blot analysis of 4kDa Aβ bands (**C**) and aggregated Aβ (> 4 kDa) (**D**) detected by antibody 6E10 showed that poly I:C (10 μg/ml) treatment did not alter intracellular levels of Aβ (1 μM) after 24 hours. (**E**) Representative western blot of triplicate determination. NS – non significant different between Aβ and poly I:C/Aβ treated samples.

Table 1:

Demographic Details of Human Brain Cases Used

Disease state (n)	Age	Sex	PMI	ApoE4	Plaques	Tangles
A: Middle temporal gyrus (Immunohistochemistry)						
ND-LP (n=15)	86.1±6.7	10M/5F	2.7±0.7	10%	2.1±2.1	3.7±2.1
ND-HP (n=10)	84.6+6.0	7M/3F	3.0±0.6	25%	9.1+1.7	2.9±.1
AD (n=11)	85.8+5.6	6M/5F	2.6±0.4	36%	14.0±1.2	12.2±2.7
B: Middle temporal gyrus – first series (RNA expression)						
ND (n=19)	79.5±11.5	15M/4F	3.0±1.1	5.5%	0.5±1.3	3.4±2.8
AD (n=24)	84.1+6.2	12M/12F	3.1±0.9	18%	13.8±1.8	13.2±3.0
C: Middle temporal gyrus – second series (RNA expression)						
ND-LP (n=14)	85.4±9.0	7M/7F	3.1±1.0	4%	1.1±1.8	5.3±2.4
ND-HP (n=13)	87.3+7.1	6M/7F	2.7±0.3	11.5%	11.4+1.9	5.1+2.0
AD (n=15)	79.7+4.6	10M/5F	3.5±0.6	30%	14.3±0.8	13.4±2.4

Abbreviations: PMI: post-mortem interval ± standard error of mean (SEM) (hr); **ApoE4**: % ApoE4 alleles; **Plaques**: Mean plaque score ± SEM (0–15); **Tangles**: Mean tangle score ± SEM (0–15); **ND:** non-demented; **AD:** Alzheimer's disease; **ND-LP:** non-demented low plaque; **ND-HP**: non-demented high plaque.

Table 2:

Details of Antibodies Used

Antigen	Antibody	Supplier	Species/Type	Application	Dilution
TLR-3	AF1847	R&D Systems	Goat/poly	IHC/WB/IP	2 μg – 0.1 μg/ul
TLR-3	MAB1847	R&D Systems	Mouse/mono	WB *	1 μg/ml
TLR-3	ab62566	Abcam	Rabbit/poly	IHC */WB *	1:2000
TLR-3	ab84991	Abcam	Rabbit/poly	WB *	1:1000
TLR-3	PA5–23510	ThermoFisher	Rabbit/poly	WB*	1:500
TLR-3	MABF72	EMD/Millipore	Mouse/mono	IHC *	1:50
Aβ	6E10	Biolegend	Mouse/mono	IHC/WB	1:2000
GFAP	556330	BD Biosciences	Mouse/mono	IHC	1:750
HLA-DR	ab166777	Abcam	Mouse/mono	IHC	1:750
IBA	019–19741	Wako	Rabbit/poly	IHC	1:1000
CD31	M0823	Agilent	Mouse/mono	IHC	1:1000
NeuN	834501	Biolegend	Mouse/mono	IHC	1:1000
p62	MAB8028	R&D Systems	Mouse/mono	IHC	1:2000
CD68	916104	Biolegend	Mouse/mono	IHC	1:1000
β actin	ab49900	Abcam	Mouse/mono-HRP	WB	1:20000

* Indicate unsatisfactory results

Table 3:

Sequences of PCR primers used for Real Time PCR analyses

Gene	Sequence	Amplicon (bp)	Ref. Seq.
TLR-2 Sense	GATGCCTACTGGGTGGAGAA	225 bp	NM_001318787.1
TLR-2 Antisense	AAAAAGACGGAAATGGGAGAA		
TLR-3 Sense	GCAACACTCCACCTCACTATC	161bp	NM_003265.2
TLR-3 Antisense	TATCCTCCAGCCCTCAAA		
TLR-4 Sense	TTGACGCAGAATGAGGAGTG	100 bp	NM_005211.3
TLR-4 Antisense	GTTGATGGGGAAGTAGTGTTTG		
TLR-9 Sense	CAGATGGAGGGGAGAAGGT	112 bp	AF245704.1
TLR-9 Antisense	AAGGTGAAGTTGAGGGTGCT		
IFN-A Sense	AAACCATCCCTGTCCTCCA	163 bp	NM_000605.3
IFN-A Antisense	ACCCCCACCCCCTGTATC		
IFN-B Sense	ACGCCGCATTGACCATCT	169 bp	NM_002176.2
IFN-B Antisense	TCTTCTTTCTCCAGTTTTTCTTCC		
IRF-3 Sense	GACAAGGAAGGAGGCGTGT	103 bp	NM_001571.5
IRF-3 Antisense	CACAGAACCAGAGGGCATAG		
IDE Sense	TTTTTCTGTGCCCCTTGTTC	202 bp	NM_004969.3
IDE Antisense	ATGCCTTCTTGGTTTGGTCT		
MME Sense	TTAGTGCCCAGCAGTCCAA	259 bp	NM_0007288.3
MME Antisense	TCAGCAATGTTTTCTCCCAGT		
β actin Sense	TCCTATGTGGGCGACGAG	242 bp	NM_001101.3
β actin Antisense	ATGGCTGGGGTGTTGAAG		